

Mean Field Analysis of Quantum Annealing Correction

Shunji Matsuura,^{1,2} Hidetoshi Nishimori,³ Tameem Albash,^{4,5,6} and Daniel A. Lidar^{5,6,7,8}

¹*Niels Bohr International Academy and Center for Quantum Devices,
Niels Bohr Institute, Copenhagen University, Blegdamsvej 17, Copenhagen, Denmark*

²*Yukawa Institute for Theoretical Physics, Kyoto University, Kyoto, Japan*

³*Department of Physics, Tokyo Institute of Technology,
Oh-okayama, Meguro-ku, Tokyo 152-8551, Japan*

⁴*Information Sciences Institute, University of Southern California, Marina del Rey, CA 90292*

⁵*Department of Physics and Astronomy, University of Southern California, Los Angeles, California 90089, USA*

⁶*Center for Quantum Information Science & Technology,
University of Southern California, Los Angeles, California 90089, USA*

⁷*Department of Electrical Engineering, University of Southern California, Los Angeles, California 90089, USA*

⁸*Department of Chemistry, University of Southern California, Los Angeles, California 90089, USA*

Quantum annealing correction (QAC) is a method that combines encoding with energy penalties and decoding to suppress and correct errors that degrade the performance of quantum annealers in solving optimization problems. While QAC has been experimentally demonstrated to successfully error-correct a range of optimization problems, a clear understanding of its operating mechanism has been lacking. Here we bridge this gap using tools from quantum statistical mechanics. We study analytically tractable models using a mean-field analysis, specifically the p -body ferromagnetic infinite-range transverse-field Ising model as well as the quantum Hopfield model. We demonstrate that for $p = 2$, where the phase transition is of second order, QAC pushes the transition to increasingly larger transverse field strengths. For $p \geq 3$, where the phase transition is of first order, QAC softens the closing of the gap for small energy penalty values and prevents its closure for sufficiently large energy penalty values. Thus QAC provides protection from excitations that occur near the quantum critical point. We find similar results for the Hopfield model, thus demonstrating that our conclusions hold in the presence of disorder.

PACS numbers: 03.67.Ac, 03.65.Yz

Quantum computing promises quantum speedups for certain computational tasks [1, 2]. Yet, this advantage is easily lost due to decoherence [3]. Quantum error correction is therefore an inevitable aspect of scalable quantum computation [4]. Quantum annealing (QA), a quantum algorithm to solve optimization problems [5–10] that is a special case of universal adiabatic quantum computing [11–15], has garnered a great deal of recent attention as it provides an accessible path to large-scale, albeit non-universal, quantum computation using present-day technology [16–19]. Specifically, QA is designed to exploit quantum effects to find the ground states of classical Ising model Hamiltonians H_C by “annealing” with a non-commuting “driver” Hamiltonian H_D . The total Hamiltonian is $H(t) = \Gamma(t)H_D + H_C$, and the time-dependent annealing parameter $\Gamma(t)$ is initially large enough that the system can be efficiently initialized in the ground state of H_D , after which it is gradually turned off, leaving only H_C at the final time. QA enjoys a large range of applicability since many combinatorial optimization problems can be formulated in terms of finding global minima of Ising spin glass Hamiltonians [20, 21]. Being simpler to implement at a large scale than other forms of quantum computing, QA may become the first method to demonstrate a widely anticipated quantum speedup, though many challenges must first be overcome [22, 23].

While QA is known to be robust against certain forms of decoherence provided the coupling to the environment

is weak [10, 24–28], error correction remains necessary in order to suppress excitations out of the ground state as well as errors associated with imperfect implementations of the desired Hamiltonian [29]. Unfortunately, unlike the circuit model of quantum computing [30], no accuracy-threshold theorem currently exists for QA or for adiabatic quantum computing. Nevertheless, error suppression and correction schemes have been proposed [31–36] and successfully implemented experimentally [37–43], resulting in significant improvements in the performance of special-purpose QA devices.

Here we focus on the quantum annealing correction (QAC) approach introduced in Ref. [37], which assumes that only the classical Hamiltonian H_C can be encoded. QAC introduces three modifications to the standard QA process. First, a repetition code is used for encoding a qubit into K (odd) physical data qubits, i.e., K independent copies of H_C are implemented given by $H_C^{(k)}$, $k = 1, \dots, K$. Second, a penalty qubit is added for each of the N encoded qubits, through which the K copies are ferromagnetically coupled with strength $\gamma > 0$, resulting in a total QAC Hamiltonian of the form:

$$H/J = - \sum_{k=1}^K (H_k^C + \Gamma H_k^D + \gamma H_k^P) , \quad (1)$$

where J is an overall energy scale which we factor out

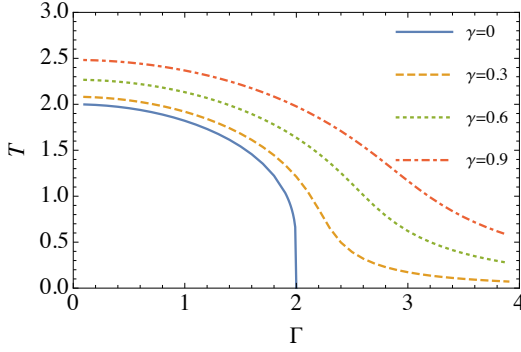


FIG. 1. The mean field phase diagram for $p = 2$ for different γ values. The lines represent second order PTs encountered along the anneal from large to small Γ values. For a fixed temperature, the critical point Γ_c increases with γ . At zero temperature, $\Gamma_c = \infty$ for $\gamma > 0$.

to make the equation dimensionless. The penalty Hamiltonian $H^P = \sum_{k=1}^K H_k^P$ represents the sum of stabilizer generators [44] of the repetition code, and it penalizes disagreements between the K copies. This allows for the suppression of errors that do not commute with the Pauli σ^z operators. Third, the observed state is decoded via majority vote on each encoded qubit, which allows for active correction of bit-flip errors.

It was shown in Refs. [37–40] that using QAC on a programmable quantum annealer [16–19] significantly increases the success probability of finding the ground state after decoding, in comparison to boosting the success probability by using the same physical resources of $K + 1$ copies of the classical Hamiltonian. This empirical observation was explained using perturbation theory and numerical analysis of small systems, where it was observed that QAC both increases the minimum gap and moves it to an earlier point in the quantum anneal (i.e., higher Γ), and recovers population from excited states via decoding.

A deeper understanding of this striking success probability enhancement result is desirable. We tackle this problem using mean-field theory, which gives us an analytical handle beyond small system sizes. Specifically, we are able to calculate the free energy associated with the QAC Hamiltonian, and in turn study the phase diagram as a function of penalty strength and transverse field strength. We do this by first studying QAC in the setting of the p -body infinite-range transverse-field Ising model, then include randomness by studying the p -body Hopfield model.

p-body Infinite-Range Ising Model encoded using QAC.—In this model the i^{th} physical qubit is replaced by the i^{th} encoded qubit, comprising K physical qubits and a penalty qubit. The terms in the QAC Hamiltonian in Eq. (1) are the infinite-range classical Hamiltonian $H_k^C = N(S_k^z)^p$, where $S_k^z \equiv \frac{1}{N} \sum_{i=1}^N \sigma_{ik}^z$, and the

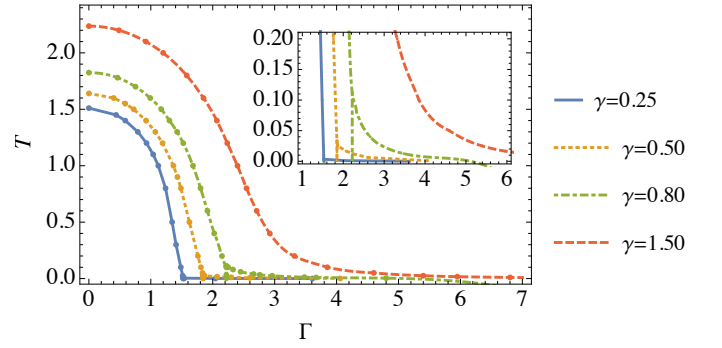


FIG. 2. The mean field phase diagram for $p = 4$ for different γ values. The lines represent first order PTs. Inset: a magnification of the low temperature region to show the presence of two first order PTs for a particular range of T and γ . At zero temperature, there exists a value γ_c such that for $\gamma > \gamma_c$, the first order PT is avoided completely, as can be seen by the case $\gamma = 1.5$.

driver and penalty Hamiltonians are given by

$$H_k^D = \sum_{i=1}^N \sigma_{ik}^x, \quad H_k^P = \sum_{i=1}^N \sigma_{ik}^z \sigma_{i0}^z, \quad (2)$$

where σ_{ik}^x and σ_{ik}^z denote the Pauli operators on physical qubit k of encoded qubit i , and σ_{i0}^z acts on the penalty qubit of encoded qubit i . Unlike in Refs. [37, 38], we do not include a transverse field on the penalty qubit, since this allows us to keep our analysis analytically tractable.

By employing the Suzuki-Trotter decomposition and the static approximation (constancy along the Trotter direction) [45–48], we find that the free energy F is given in the thermodynamic limit ($N \rightarrow \infty$) by

$$F/J = (p-1) \sum_{k=1}^K m_k^p - \frac{1}{\beta} \ln \left(e^{\sum_{k=1}^K \beta \sqrt{(\gamma - p m_k^{p-1})^2 + \Gamma^2}} + e^{\sum_{k=1}^K \beta \sqrt{(\gamma + p m_k^{p-1})^2 + \Gamma^2}} \right) \quad (3a)$$

$$\xrightarrow{\beta \rightarrow \infty} \sum_{k=1}^K \left[(p-1) m_k^p - \sqrt{(\gamma + p |m_k|^{p-1})^2 + \Gamma^2} \right], \quad (3b)$$

where m_k is the Hubbard-Stratonovich field [49] that also plays the role of an order parameter, and $\beta = (k_B T)^{-1}$ is the inverse temperature. This free energy for the infinite-range model appropriately reflects quantum effects, i.e., the eigenstates are not classical product states, as further commented on in Sec. I of the Supplementary Material (SM). The dominant contribution to F comes from the saddle-point of the partition function $Z = \exp(-\beta N F)$, which provides a consistency equation for m_k . The solution that minimizes the free energy has all K copies with the same spin configuration, i.e., $m_k = m \forall k$, which is the stable state. Metastable solutions exist where $m_k = m$

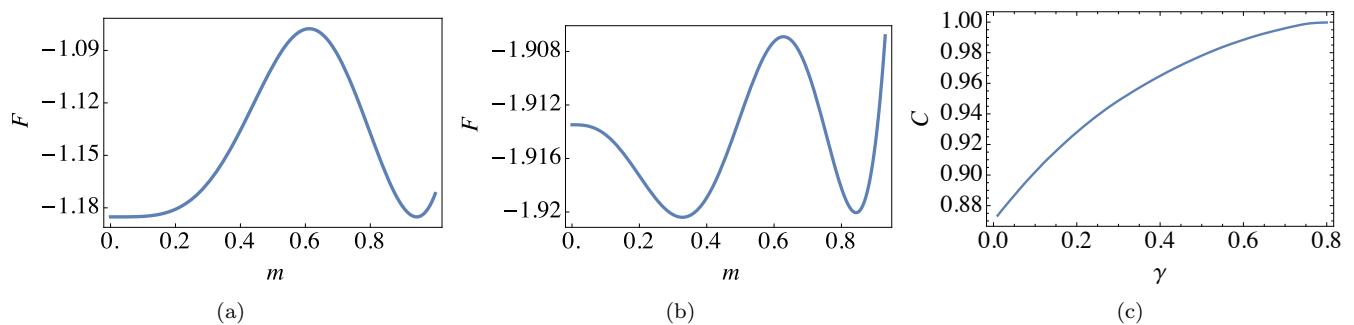


FIG. 3. Results for $p = 4$, $T \rightarrow 0$, and $J = 1$. (a) The free energy for $\gamma = 0$ at the critical point $\Gamma_c = 1.185$. The two degenerate global minima are at $m = 0$ and 0.943 . (b) The free energy for $\gamma = 0.5$ at the critical point $\Gamma_c = 1.847$. Now the two degenerate global minima are at $m = 0.328$ and 0.844 . For $\gamma = 0.5$, the symmetric point $m = 0$ is metastable and the global minimum has non-zero magnetization even for large Γ . This minimum continuously moves to $m = 0.328$ along the anneal, and then discontinuously jumps to $m = 0.844$ at $\Gamma_c = 1.847$. (c) The coefficient C associated with the scaling of the gap in the symmetric subspace ($\Delta \sim C^N$). C increases monotonically towards unity as a function of γ .

for $k = 1, \dots, \kappa$ and $m_k = -m$ for $k = \kappa + 1, \dots, K$, which represent local minima and are decodable errors provided $\kappa > K/2$. Additional details of the derivation of F can be found in the SM.

When $p = 2$, it is well known that for $\gamma = 0$ (where the K copies are decoupled) there is a second order PT from a symmetric (paramagnetic) phase to a symmetry-broken (ferromagnetic) phase, at $\Gamma_c = 2$ [50]. However, as shown in Fig. 6, as γ increases, the PT is pushed to increasingly larger Γ_c values for fixed β , until, as $\beta \rightarrow \infty$ also $\Gamma_c \rightarrow \infty$ for any $\gamma > 0$. This means that in the zero temperature limit the PT is effectively *avoided* for any $\gamma > 0$, while for $T > 0$ as γ is increased the system spends an increasingly larger fraction of the anneal in the symmetry-broken phase.

For $p > 2$, there is a first order PT for $\gamma = 0$ [50]. We show the $p = 4$ phase diagram in Fig. 7, for different values of γ . We find several interesting regimes that we observe generically for $p > 2$. In the zero temperature limit, there is a single first order PT between $m = 0$ and $m = m_{\text{large}}$ that persists even for small γ , and the associated Γ_c increases monotonically as a function of γ , as $\Gamma_c \approx 1.4\gamma + 1.2$. However, the PT *disappears* for $\gamma > \gamma_c(p)$, where $\gamma_c(p) \approx 0.46p - 1$ (see the SM). In general, such a result should be taken as an indication that the penalty is too strong, in the sense that it overwhelmed H_C and has potentially turned a hard instance into an easy one.

For $T, \gamma \gtrsim 0$ we observe *two* first order PTs. The first is between $m = 0$ and $m = m_{\text{small}}$, followed by a PT between m_{small} and m_{large} at a smaller Γ . If γ is made larger than a critical value of γ_{c2} at these low temperatures, then only the former PT survives, and m_{small} smoothly moves to m_{large} as Γ is decreased. Further details are provided in the SM.

The penalty term also changes the first order PT quantitatively. In Figs. 3(a) and 3(b), we show the free ener-

gies at the critical points for $\gamma = 0$ and 0.5 in the $T \rightarrow 0$ limit. The penalty term reduces the width and the height of the potential barrier, thus increasing the probability that the system will tunnel from the left well (small m ; global minimum for $\Gamma > \Gamma_c$) to the right well (large m ; global minimum for $\Gamma < \Gamma_c$). This is similar to the reduction and elimination of the barrier heights when different driver Hamiltonians are used [51–53].

We can relate the reduction of the width and the height of the mean-field free energy barrier to the softening of the energy gap between the ground state and the first excited state. We use our earlier finding that in the $T \rightarrow 0$ limit the penalty qubits are locked into alignment with the ground state of $H_C^{(k)}$. This configuration of penalty qubits defines a particular sector of the Hilbert space of H , which contains the global ground state of H . We can thus confine our analysis to one of the two corresponding sectors, i.e., where $\sigma_{i0}^z = +1 \forall i$; at $T = 0$ and in the absence of a transverse field there is no mechanism to flip the penalty qubits. This decouples the K copies and the penalty becomes a global field in the z -direction. The Hamiltonian H restricted to this sector is invariant under all permutations of the logical qubit index i . Therefore, if we initialize the system in this symmetric subspace it will remain there under the unitary evolution. This symmetric subspace is spanned by the Dicke states (eigenstates of the collective angular momentum operators with maximal total angular momentum), and the dimensionality of each of the K copies is reduced from 2^N to $N + 1$ (see the SM). In the Dicke state basis the Hamiltonian is tridiagonal and can be efficiently diagonalized [47]. Doing so for sufficiently large N 's allows us to extract the scaling of the minimum gap Δ in the symmetric subspace. We show for the case of $p = 4$ that $\Delta \sim C^N$, with C given in Fig. 3(c). As γ increases C increases as well, asymptoting to 1 for large γ , at which point the gap is constant. This softening of the closing of the gap with γ is obviously a

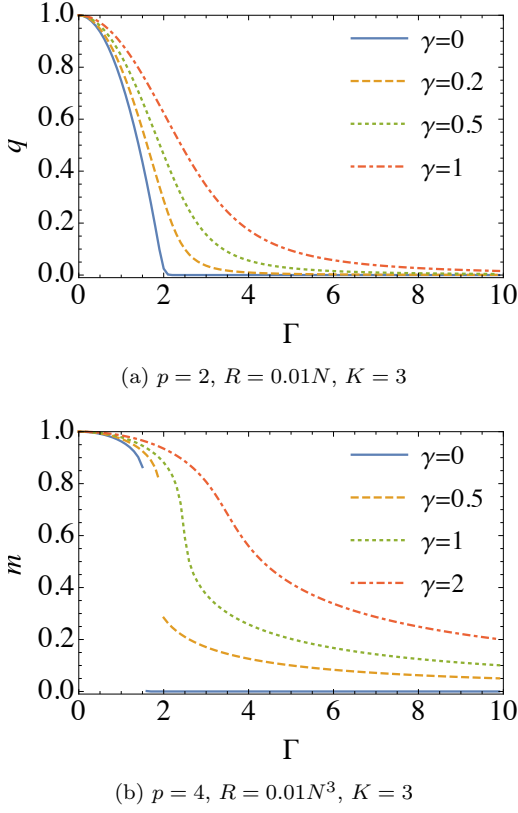


FIG. 4. (a) The q value at the free energy extremum for the Hopfield many-patterns case with $p = 2$, $R = 0.01N$, and $K = 3$ under the replica symmetric ansatz. For $\gamma \neq 0$, the system remains in the symmetry-broken phase at least up to $\Gamma = 10$, while for $\gamma = 0$ the symmetric phase is present for $\Gamma \gtrsim 2.2$. (b) The m value at the free energy extremum for the Hopfield many-patterns case with $p = 4$, $R = 0.01N^3$ and $K = 3$. For $\gamma = 0$, there is a first order transition around $\Gamma = 1.6$, and the extremum jumps discontinuously from $m = 0.86$ to $m = 0$. For $\gamma = 0.5$, there is again a discontinuous jump in the value of m but it does not reach $m = 0$. For $\gamma = 1, 2$ a discontinuity is not observed suggesting that the first order PT disappears or is at least weakened considerably by the penalty term.

desirable aspect of QAC, since it reduces the sensitivity to excitations and in turn implies an enhancement of the success probability of the QA algorithm.

Hopfield model encoded using QAC.—The ferromagnetic model considered above has a trivial classical ground state. To understand whether a more challenging computational problem exhibiting randomness affects our conclusions, we now consider the quantum Hopfield model [54, 55], but limit ourselves to the $T = 0$ case for simplicity. The encoded Hamiltonian of the Hopfield model is again given by Eq. (1), and the driver and penalty Hamiltonians are given in Eq. (2). The classical Hamiltonian is $H_k^C = N \sum_{\mu=1}^R \left(\frac{1}{N} \sum_{i=1}^N \xi_i^\mu \sigma_{ik}^z \right)^p$, where the R “patterns” ξ_i^μ (indexed by μ) take random values ± 1 . The Hubbard-Stratonovich field is now labeled by

m_k^μ . Note that the p -body infinite-range Ising model is the special case with $R = 1$ and $\xi_i^\mu \equiv 1$.

Let us first consider the case of a finite number of patterns, i.e., $m_k^\mu = m_k$ for $0 \leq \mu \leq l$ and $m_k^\mu = 0$ for $\mu \geq l+1$. We then find that the free energy is minimized by $l = 1$ for all Γ (see SM) and is identical to Eq. (28); thus the conclusions obtained above for the uniform ferromagnetic case apply in this case as well.

Next, we consider the “many-patterns” case, where the number of patterns scales as $R = \mathcal{O}(N^{p-1})$ (ensuring extensivity). In this case, the free energy under the ansatz of replica symmetry [56] is a function of two order parameters: the one- and two-point spin correlation functions m and q . Both order parameters are relevant for determining the phase, and hence the complexity, of the Ising Hamiltonian. Details can be found in the SM.

Our results are illustrated in Fig. 4. For $p = 2$ and $\gamma = 0$, the extremum of the free energy is at the symmetric point $(m, q) = (0, 0)$ for large Γ and moves continuously to the symmetry-broken phase with nonzero q as Γ goes below Γ_c . For finite γ , the system is in the symmetry-broken phase even for large Γ and is never at $(m, q) = (0, 0)$ [see Fig. 4(a)]. For $p = 4$ and $\gamma = 0$, there is a discontinuous jump in (m, q) as a function of Γ , indicating the presence of a first-order PT. For finite values of γ , the discontinuity is smaller in magnitude, and it eventually disappears as γ increases [see Fig. 4(b)]. These qualitative features are the same as those observed in the uniform ferromagnetic case above. Therefore, QAC improves the success probability of the QA algorithm even in the presence of certain types of randomness. We note that replica symmetry breaking may change some of the results [56]. For example, the PT for $p = 2$ may persist up to a finite value of γ but will disappear for sufficiently large γ . We can trust at least the qualitative aspects of our result that effects of PTs become less prominent under the presence of the penalty term, which would enhance the performance of QA.

Conclusions.—We have demonstrated that in the thermodynamic limit, depending on the penalty strength γ , QAC either softens or prevents the closing of the minimum energy gap. In the latter case the associated PT is avoided in the $T \rightarrow 0$ limit, while in the $T > 0$ setting only the conclusion that the gap-closing is softened survives. Indeed, it is unreasonable to expect that QAC changes the computational complexity class of the optimization problem of the corresponding QA process. This would help to explain the increase in success probability witnessed in QAC experiments [37–40].

An important aspect of QAC that is absent in the analysis presented here is the decoding step, which is known to lead to an optimal penalty strength [37–40]; this aspect may emerge as we attempt to keep decodable metastable solutions closer to the global minimum than undecodable solutions, and will be addressed in future work.

S.M. and H.N. thank Y. Seki for his useful com-

ments. D.A.L. and T.A. acknowledge support under ARO Grant No. W911NF-12-1-0523, ARO MURI Grant No. W911NF-11-1-0268, NSF Grant No. CCF-1551064, and partial support from Fermi Research Alliance, LLC under Contract No. DE-AC02-07CH11359 with the United States Department of Energy. H.N. acknowledges support by JSPS KAKENHI Grant No. 26287086.

-
- [1] A. M. Childs and W. van Dam, *Reviews of Modern Physics* **82**, 1 (2010).
- [2] S. Jordan, “Quantum algorithm zoo,” .
- [3] H.-P. Breuer and F. Petruccione, *The Theory of Open Quantum Systems* (Oxford University Press, 2002).
- [4] D. Lidar and T. Brun, eds., *Quantum Error Correction* (Cambridge University Press, Cambridge, UK, 2013).
- [5] T. Kadowaki and H. Nishimori, *Phys. Rev. E* **58**, 5355 (1998).
- [6] P. Ray, B. K. Chakrabarti, and A. Chakrabarti, *Phys. Rev. B* **39**, 11828 (1989).
- [7] J. Brooke, D. Bitko, T. F., Rosenbaum, and G. Aeppli, *Science* **284**, 779 (1999).
- [8] J. Brooke, T. F. Rosenbaum, and G. Aeppli, *Nature* **413**, 610 (2001).
- [9] G. E. Santoro, R. Martoňák, E. Tosatti, and R. Car, *Science* **295**, 2427 (2002).
- [10] W. M. Kaminsky, S. Lloyd, and T. P. Orlando, “Quantum computing and quantum bits in mesoscopic systems,” (Springer, New York, 2004) Chap. 25, pp. 229–236.
- [11] E. Farhi, J. Goldstone, S. Gutmann, and M. Sipser, *arXiv:quant-ph/0001106* (2000).
- [12] D. Aharonov, W. van Dam, J. Kempe, Z. Landau, S. Lloyd, and O. Regev, *SIAM J. Comput.* **37**, 166 (2007).
- [13] A. Mizel, D. A. Lidar, and M. Mitchell, *Phys. Rev. Lett.* **99**, 070502 (2007).
- [14] D. Gosset, B. M. Terhal, and A. Vershynina, *Physical Review Letters* **114**, 140501 (2015).
- [15] S. Lloyd and B. Terhal, *arXiv:1509.01278* (2015).
- [16] M. W. Johnson, P. Bunyk, F. Maibaum, E. Tolkacheva, A. J. Berkley, E. M. Chapple, R. Harris, J. Johansson, T. Lanting, I. Perminov, E. Ladizinsky, T. Oh, and G. Rose, *Superconductor Science and Technology* **23**, 065004 (2010).
- [17] A. J. Berkley, M. W. Johnson, P. Bunyk, R. Harris, J. Johansson, T. Lanting, E. Ladizinsky, E. Tolkacheva, M. H. S. Amin, and G. Rose, *Superconductor Science and Technology* **23**, 105014 (2010).
- [18] R. Harris, M. W. Johnson, T. Lanting, A. J. Berkley, J. Johansson, P. Bunyk, E. Tolkacheva, E. Ladizinsky, N. Ladizinsky, T. Oh, F. Cioata, I. Perminov, P. Spear, C. Enderud, C. Rich, S. Uchaikin, M. C. Thom, E. M. Chapple, J. Wang, B. Wilson, M. H. S. Amin, N. Dickson, K. Karimi, B. Macready, C. J. S. Truncik, and G. Rose, *Phys. Rev. B* **82**, 024511 (2010).
- [19] P. I. Bunyk, E. M. Hoskinson, M. W. Johnson, E. Tolkacheva, F. Altomare, A. Berkley, R. Harris, J. P. Hilton, T. Lanting, A. Przybysz, and J. Whittaker, *Applied Superconductivity, IEEE Transactions on, Applied Superconductivity, IEEE Transactions on* **24**, 1 (Aug. 2014).
- [20] E. Farhi, J. Goldstone, S. Gutmann, J. Lapan, A. Lundgren, and D. Preda, *Science* **292**, 472 (2001).
- [21] A. Lucas, *Front. Phys.* **2**, 5 (2014).
- [22] T. F. Rønnow, Z. Wang, J. Job, S. Boixo, S. V. Isakov, D. Wecker, J. M. Martinis, D. A. Lidar, and M. Troyer, *Science* **345**, 420 (2014).
- [23] S. Aaronson, *Nat Phys* **11**, 291 (2015).
- [24] A. M. Childs, E. Farhi, and J. Preskill, *Phys. Rev. A* **65**, 012322 (2001).
- [25] M. S. Sarandy and D. A. Lidar, *Phys. Rev. Lett.* **95**, 250503 (2005).
- [26] J. Aberg, D. Kult, and E. Sjöqvist, *Physical Review A* **72**, 042317 (2005).
- [27] J. Roland and N. J. Cerf, *Phys. Rev. A* **71**, 032330 (2005).
- [28] T. Albash and D. A. Lidar, *Physical Review A* **91**, 062320 (2015).
- [29] K. C. Young, M. Sarovar, and R. Blume-Kohout, *Phys. Rev. X* **3**, 041013 (2013).
- [30] J. Preskill, *Quant. Inf. Comput.* **13**, 181 (2013).
- [31] S. P. Jordan, E. Farhi, and P. W. Shor, *Phys. Rev. A* **74**, 052322 (2006).
- [32] D. A. Lidar, *Phys. Rev. Lett.* **100**, 160506 (2008).
- [33] G. Quiroz and D. A. Lidar, *Phys. Rev. A* **86**, 042333 (2012).
- [34] K. C. Young, R. Blume-Kohout, and D. A. Lidar, *Phys. Rev. A* **88**, 062314 (2013).
- [35] A. Ganti, U. Onunkwo, and K. Young, *Phys. Rev. A* **89**, 042313 (2014).
- [36] A. Mizel, *arXiv:1403.7694* (2014).
- [37] K. L. Pudenz, T. Albash, and D. A. Lidar, *Nat. Commun.* **5**, 3243 (2014).
- [38] K. L. Pudenz, T. Albash, and D. A. Lidar, *Phys. Rev. A* **91**, 042302 (2015).
- [39] W. Vinci, T. Albash, G. Paz-Silva, I. Hen, and D. A. Lidar, *arXiv:1507.02658* (2015).
- [40] A. Mishra, T. Albash, and D. Lidar, *arXiv:1508.02785* (2015).
- [41] D. Venturelli, S. Mandrà, S. Knysh, B. O’Gorman, R. Biswas, and V. Smelyanskiy, *arXiv:1406.7553* (2014).
- [42] A. D. King and C. C. McGeoch, *arXiv:1410.2628* (2014).
- [43] A. Perdomo-Ortiz, J. Fluegeman, R. Biswas, and V. N. Smelyanskiy, *arXiv:1503.01083* (2015).
- [44] D. Gottesman, *Phys. Rev. A* **54**, 1862 (1996).
- [45] L. Chayes, N. Crawford, D. Ioffe, and A. Levit, *Journal of Statistical Physics* **133**, 131 (2008).
- [46] F. Krzakala, A. Rosso, G. Semerjian, and F. Zamponi, *Phys. Rev. B* **78**, 134428 (2008).
- [47] T. Jörg, F. Krzakala, J. Kurchan, A. C. Maggs, and J. Pujos, *EPL (Europhysics Letters)* **89**, 40004 (2010).
- [48] S. Suzuki, J. Inoue, and B. Chakrabarti, *Quantum Ising Phases and Transitions in Transverse Ising Models*, 2nd ed., Lecture Notes in Physics, Vol. 862 (Springer Verlag, Berlin, 2013).
- [49] J. Hubbard, *Physical Review Letters* **3**, 77 (1959).
- [50] M. Filippone, S. Dusuel, and J. Vidal, *Phys. Rev. A* **83**, 022327 (2011).
- [51] E. Farhi, J. Goldstone, and S. Gutmann, *arXiv:quant-ph/0208135* (2002).
- [52] A. Boulatov and V. N. Smelyanskiy, *Phys. Rev. A* **68**, 062321 (2003).
- [53] Y. Seki and H. Nishimori, *Phys. Rev. E* **85**, 051112 (2012).
- [54] H. Nishimori and Y. Nonomura, *Journal of the Physical*

- Society of Japan **65**, 3780 (1996).
- [55] Y. Seki and H. Nishimori, *Journal of Physics A: Mathematical and Theoretical* **48**, 335301 (2015).
- [56] H. Nishimori, *Statistical Physics of Spin Glasses and Information Processing: An Introduction* (Oxford University Press, Oxford, UK, 2001).
- [57] B. Seoane and H. Nishimori, *Journal of Physics A: Mathematical and Theoretical* **45**, 435301 (2012).
- [58] A. J. Bray and M. A. Moore, *Journal of Physics C: Solid State Physics* **13**, L655 (1980).
- [59] The initial state is $|+\rangle \cdots |+\rangle$. To see that it belongs to

- the $\{|J = \frac{N}{2}, M\rangle\}$ subspace note that, e.g., for $N = 2$, the singlet subspace $|J = 0, M = 0\rangle$ is the antisymmetric state $\frac{1}{\sqrt{2}}(|01\rangle - |10\rangle)$, while the initial state is $\frac{1}{2}(|00\rangle + |01\rangle + |10\rangle + |11\rangle)$, which belongs to the triplet subspace spanned by $|J = 1, M = -1, 0, 1\rangle = \{|00\rangle, \frac{1}{\sqrt{2}}(|01\rangle + |10\rangle), |11\rangle\}$.
- [60] L. Mandel and E. Wolf, *Optical Coherence and Quantum Optics* (Cambridge University Press, New York, 1995).
- [61] D. J. Amit, H. Gutfreund, and H. Sompolinsky, *Annals of Physics* **173**, 30 (1987).

Supplementary Material for “Mean Field Analysis of Quantum Annealing Correction”

In the main text we were concerned with Hamiltonians of the form

$$H/J = H^x + H^z, \quad (4)$$

where J has dimensions of energy, and

$$H^x = -\Gamma \sum_{k=1}^K H_k^D, \quad (5)$$

$$H^z = -\sum_{k=1}^K (H_k^C + \gamma H_k^P). \quad (6)$$

H^x involves only σ^x -type Pauli operators and H^z involves only σ^z -type Pauli operators. Note that both γ and Γ are dimensionless since we have already factored out the energy scale J . The driver and penalty Hamiltonians are

$$H_k^D = N \left(S_k^x + \frac{\varepsilon}{K} S_0^x \right), \quad S_k^x \equiv \frac{1}{N} \sum_{i=1}^N \sigma_{ik}^x \quad (7a)$$

$$H_k^P = \sum_{i=1}^N \sigma_{ik}^z \sigma_{i0}^z. \quad (7b)$$

Throughout we use σ_{ik}^α to denote the α -type Pauli operator acting on physical qubit k of encoded qubit i . The term σ_{i0}^x represents the transverse field on the penalty qubit shared by the K copies, which we assume has magnitude $\varepsilon \geq 0$. We keep this term for now, though in the main text we consider only the $\varepsilon = 0$ case. The case with $\varepsilon = 0$ is illustrated in Fig. 5 for a chain.

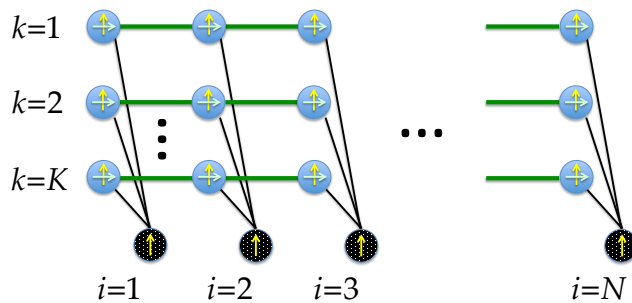


FIG. 5. Schematic of the QAC scheme for a chain. Filled blue circles represent physical data qubits, dotted black circles are the corresponding penalty qubits, coupled via the thin black lines. Thick green lines represent couplings in the classical Hamiltonian H_k^C , up-pointing arrows are longitudinal local fields in H_k^C , sideways-pointing arrows are transverse fields from the driver Hamiltonian (data qubits only).

The classical (problem) Hamiltonian is either the p -body infinite-range ferromagnetic Ising model

$$H_k^C = N(S_k^z)^p, \quad S_k^z \equiv \frac{1}{N} \sum_{i=1}^N \sigma_{ik}^z, \quad (8)$$

or the Hopfield model

$$H_k^C = N \sum_{\mu=1}^R (S_{k,\xi^\mu}^z)^p, \quad S_{k,\xi^\mu}^z \equiv \frac{1}{N} \sum_{i=1}^N \xi_i^\mu \sigma_{ik}^z. \quad (9)$$

We are interested in the partition function

$$Z = \text{Tr} e^{-\beta H} = \text{Tr} e^{-\beta J[H^x + H^z]} = \text{Tr} e^{-\beta[H^x + H^z]}, \quad (10)$$

where $\beta = J\beta$ is the dimensionless inverse temperature.

From here on, our calculations are similar to Appendix A of Ref. [57]. We write the partition function explicitly as

$$Z = \sum_{\{\sigma^z\}} \langle \{\sigma^z\} | \exp[-\beta(H^z + H^x)] | \{\sigma^z\} \rangle = \lim_{M \rightarrow \infty} Z_M, \quad (11)$$

where $\sum_{\{\sigma^z\}}$ is a sum over all possible $2^{(K+1)N}$ spin configurations in the z basis, and $|\{\sigma^z\}\rangle = \otimes_{i=1}^N \otimes_{k=0}^K |\sigma_{ik}^z\rangle$. Z_M is determined using the Trotter-Suzuki formula $e^{A+B} = \lim_{M \rightarrow \infty} (e^{A/M} e^{B/M})^M$:

$$Z_M = \sum_{\{\sigma^z\}} \langle \{\sigma^z\} | \left(\exp\left[-\frac{\beta}{M} H^z\right] \exp\left[-\frac{\beta}{M} H^x\right] \right)^M | \{\sigma^z\} \rangle. \quad (12)$$

We introduce M copies of the identity operator closure relations $I(\alpha) = \sum_{\{\sigma^z(\alpha)\}} |\{\sigma^z(\alpha)\}\rangle \langle \{\sigma^z(\alpha)\}|$, each labeled by the Trotter time α :

$$Z_M = \prod_{\alpha=1}^M \sum_{\{\sigma^z(\alpha)\}} \langle \{\sigma^z(\alpha)\} | \left(\exp\left[-\frac{\beta}{M} H^z\right] \exp\left[-\frac{\beta}{M} H^x\right] \right) | \{\sigma^z(\alpha+1)\} \rangle, \quad (13)$$

where $|\{\sigma^z(M+1)\}\rangle \equiv |\{\sigma^z(1)\}\rangle$; M is known as the Trotter number. Likewise we introduce M copies of the identity operator closure relations $I(\alpha) = \sum_{\{\sigma^x(\alpha)\}} |\{\sigma^x(\alpha)\}\rangle \langle \{\sigma^x(\alpha)\}|$:

$$Z_M = \prod_{\alpha=1}^M \sum_{\{\sigma^{x,z}(\alpha)\}} \langle \{\sigma^z(\alpha)\} | \exp\left[-\frac{\beta}{M} H^z\right] | \{\sigma^x(\alpha)\} \rangle \langle \{\sigma^x(\alpha)\} | \exp\left[-\frac{\beta}{M} H^x\right] | \{\sigma^z(\alpha+1)\} \rangle \quad (14a)$$

$$= \prod_{\alpha=1}^M \sum_{\{\sigma^{x,z}(\alpha)\}} \exp\left[-\frac{\beta}{M} H^z(\alpha)\right] \langle \{\sigma^z(\alpha)\} | \{\sigma^x(\alpha)\} \rangle \exp\left[-\frac{\beta}{M} H^x(\alpha)\right] \langle \{\sigma^x(\alpha)\} | \{\sigma^z(\alpha+1)\} \rangle \quad (14b)$$

$$= \prod_{\alpha=1}^M \sum_{\{\sigma^{x,z}(\alpha)\}} \exp\left[-\frac{\beta}{M} (H^z(\alpha) + H^x(\alpha))\right] \langle \{\sigma^z(\alpha)\} | \{\sigma^x(\alpha)\} \rangle \langle \{\sigma^x(\alpha)\} | \{\sigma^z(\alpha+1)\} \rangle. \quad (14c)$$

The notation $\{\sigma^{x,z}(\alpha)\}$ is shorthand for $\{\{\sigma_{ik}^x(\alpha), \sigma_{ik}^z(\alpha)\}_{k=0}^K\}_{i=1}^N$, and

$$\langle \{\sigma^z(\alpha)\} | \{\sigma^x(\alpha)\} \rangle \langle \{\sigma^x(\alpha)\} | \{\sigma^z(\alpha+1)\} \rangle = \prod_{i=1}^N \prod_{k=0}^K \langle \sigma_{ik}^z(\alpha) | \sigma_{ik}^x(\alpha) \rangle \langle \sigma_{ik}^x(\alpha) | \sigma_{ik}^z(\alpha+1) \rangle. \quad (15)$$

Note that this allowed us to replace the operators H^x and H^z by c-numbers $H^x(\alpha)$ and $H^z(\alpha)$.

We now specialize to the two models considered in the main text.

p -BODY INFINITE-RANGE FERROMAGNETIC ISING MODEL

In this case

$$H^z(\alpha) = - \sum_{k=1}^K [N(S_k^z(\alpha))^p + \gamma H_k^P(\alpha)] . \quad (16)$$

We rewrite the p -body interaction in terms of one-body interactions by introducing auxiliary Hubbard-Stratonovich fields $m_{k\alpha}$ and $m'_{k\alpha}$, which play the role of an order parameter and a Lagrange multiplier respectively. This is done by successively using the elementary δ function identities

$$f(a) = \int_{-\infty}^{\infty} f(m_{k\alpha}) \delta(m_{k\alpha} - a) dm_{k\alpha}, \quad \delta(m_{k\alpha} - a) = \frac{1}{2\pi} \int_{-\infty}^{\infty} e^{i(m_{k\alpha} - a)m'_{k\alpha}} dm'_{k\alpha}, \quad (17)$$

with $a = S_k^z(\alpha)$, namely, continuing from Eq. (14c):

$$Z_M = \prod_{\alpha=1}^M \sum_{\{\sigma^{x,z}(\alpha)\}} \prod_{k=1}^K \left\{ \int dm_{k\alpha} \delta(m_{k\alpha} - S_k^z(\alpha)) \exp \left[\frac{\beta}{M} (Nm_{k\alpha}^p + \gamma H_k^P(\alpha)) \right] \right\} \exp \left[\frac{\beta\Gamma}{M} \sum_{k=1}^K H_k^D(\alpha) \right] \\ \times \langle \{\sigma^z(\alpha)\} | \{\sigma^x(\alpha)\} \rangle \langle \{\sigma^x(\alpha)\} | \{\sigma^z(\alpha+1)\} \rangle \quad (18a)$$

$$= \prod_{\alpha=1}^M \sum_{\{\sigma^{x,z}(\alpha)\}} \prod_{k=1}^K \left\{ \int dm_{k\alpha} \int \frac{dm'_{k\alpha}}{2\pi} \exp [im'_{k\alpha} (m_{k\alpha} - S_k^z(\alpha))] \exp \left[\frac{\beta N}{M} m_{k\alpha}^p + \frac{\beta\gamma}{M} H_k^P(\alpha) + \frac{\beta\Gamma}{M} H_k^D(\alpha) \right] \right\} \\ \times \langle \{\sigma^z(\alpha)\} | \{\sigma^x(\alpha)\} \rangle \langle \{\sigma^x(\alpha)\} | \{\sigma^z(\alpha+1)\} \rangle . \quad (18b)$$

To proceed, we use the static approximation [46, 58], i.e., $m_{k\alpha} \mapsto m_k$ and $m'_{k\alpha} \mapsto m'_k$. We also make a change of variables $m'_k = \frac{N}{M} \tilde{m}_k$. The partition function is now given by:

$$Z_M = \prod_{\alpha=1}^M \sum_{\{\sigma^{x,z}(\alpha)\}} \prod_{k=1}^K \left\{ \int dm_k \int \frac{Nd\tilde{m}_k}{2\pi M} \exp \left[i \frac{N}{M} \tilde{m}_k (m_k - S_k^z(\alpha)) \right] \exp \left[\frac{\beta N}{M} m_k^p + \frac{\beta\gamma}{M} H_k^P(\alpha) + \frac{\beta\Gamma}{M} H_k^D(\alpha) \right] \right\} \\ \times \langle \{\sigma^z(\alpha)\} | \{\sigma^x(\alpha)\} \rangle \langle \{\sigma^x(\alpha)\} | \{\sigma^z(\alpha+1)\} \rangle \quad (19a)$$

$$= \prod_{k=1}^K \int dm_k \int d\tilde{m}_k \exp (iN\tilde{m}_k m_k + \beta N m_k^p) \prod_{\alpha=1}^M \sum_{\{\sigma^{x,z}(\alpha)\}} \prod_{k=1}^K \exp \left[-i\tilde{m}_k \frac{N}{M} S_k^z(\alpha) + \frac{\beta\gamma}{M} H_k^P(\alpha) + \frac{\beta\Gamma}{M} H_k^D(\alpha) \right] \\ \times \langle \{\sigma^z(\alpha)\} | \{\sigma^x(\alpha)\} \rangle \langle \{\sigma^x(\alpha)\} | \{\sigma^z(\alpha+1)\} \rangle \quad (19b)$$

$$\rightarrow \prod_{k=1}^K \int dm_k \int d\tilde{m}_k \exp (iN\tilde{m}_k m_k + \beta N m_k^p) \text{Tr} \prod_{k=1}^K \exp \left[-i\tilde{m}_k N S_k^z + \beta\gamma H_k^P + \beta\Gamma H_k^D \right], \quad (19c)$$

where in the last line we took $M \rightarrow \infty$ and rewrote $\prod_{\alpha=1}^M \sum_{\{\sigma^{x,z}(\alpha)\}}$ in terms of the trace. Note that we replaced $\frac{Nd\tilde{m}_k}{2\pi M}$ by $d\tilde{m}_k$; the factor $\frac{N}{2\pi M}$ will ultimately not matter since we are interested (below) in the saddle points of the integrand. The same result can be derived using the path-integral formulation of quantum mechanics under the static approximation, i.e., with imaginary-time independent variables. It is also worth noting that quantum fluctuations are appropriately taken into account even after the static approximation, as reflected in the α -dependence of the Hamiltonians in Eqs. (19a) and (19b).

Now note that

$$\text{Tr} \prod_{k=1}^K \exp (-i\tilde{m}_k N S_k^z + \beta\gamma H_k^P + \beta\Gamma H_k^D) = \text{Tr} \prod_{i=1}^N \prod_{k=1}^K \exp \left[-i\tilde{m}_k \sigma_{ik}^z + \beta\gamma \sigma_{ik}^z \sigma_{i0}^z + \beta\Gamma \left(\sigma_{ik}^x + \frac{\varepsilon}{K} \sigma_{i0}^x \right) \right] \quad (20a)$$

$$= \left(\text{Tr} \prod_{k=1}^K \exp \left[-i\tilde{m}_k \sigma_k^z + \beta\gamma \sigma_k^z \sigma_0^z + \beta\Gamma \left(\sigma_k^x + \frac{\varepsilon}{K} \sigma_0^x \right) \right] \right)^N, \quad (20b)$$

since terms with different values of i commute.

At this point we set $\varepsilon = 0$. This amounts to treating the penalty qubit as a classical Ising spin, and allows us to trace it out:

$$Z = \prod_{k=1}^K \int dm_k \int d'\tilde{m}_k e^{N(im_k m_k + \beta m_k^p)} \left(\text{Tr} \prod_{k=1}^K e^{-i\tilde{m}_k \sigma_k^z + \beta \gamma \sigma_k^z + \beta \Gamma \sigma_k^x} + \text{Tr} \prod_{k=1}^K e^{-i\tilde{m}_k \sigma_k^z - \beta \gamma \sigma_k^z + \beta \Gamma \sigma_k^x} \right)^N. \quad (21)$$

The residual term from tracing out the penalty qubit acts as a local field. The eigenvalues of the operators in the remaining exponents are $\pm \sqrt{(\beta \gamma \pm i\tilde{m}_k)^2 + (\beta \Gamma)^2}$ so we can perform the trace to give

$$Z = \prod_{k=1}^K \int dm_k \int d'\tilde{m}_k e^{N(im_k \tilde{m}_k + \beta m_k^p)} \times \left(\prod_{k=1}^K \left(e^{\sqrt{(\beta \gamma - i\tilde{m}_k)^2 + (\beta \Gamma)^2}} + e^{-\sqrt{(\beta \gamma - i\tilde{m}_k)^2 + (\beta \Gamma)^2}} \right) + \prod_{k=1}^K \left(e^{\sqrt{(\beta \gamma + i\tilde{m}_k)^2 + (\beta \Gamma)^2}} + e^{-\sqrt{(\beta \gamma + i\tilde{m}_k)^2 + (\beta \Gamma)^2}} \right) \right)^N. \quad (22)$$

In the large β limit, the dominant contribution is from the positive power terms:

$$Z \approx \prod_{k=1}^K \int dm_k \int d'\tilde{m}_k e^{N(im_k \tilde{m}_k + \beta m_k^p)} \left(\prod_{k=1}^K e^{\sqrt{(\beta \gamma - i\tilde{m}_k)^2 + (\beta \Gamma)^2}} + \prod_{k=1}^K e^{\sqrt{(\beta \gamma + i\tilde{m}_k)^2 + (\beta \Gamma)^2}} \right)^N \quad (23a)$$

$$= \prod_{k=1}^K \int dm_k \int d'\tilde{m}_k \exp \left\{ N \left[\sum_{k=1}^K (im_k \tilde{m}_k + \beta m_k^p) + \log \left(e^{\sum_{k=1}^K \sqrt{(\beta \gamma - i\tilde{m}_k)^2 + (\beta \Gamma)^2}} + e^{\sum_{k=1}^K \sqrt{(\beta \gamma + i\tilde{m}_k)^2 + (\beta \Gamma)^2}} \right) \right] \right\}. \quad (23b)$$

In the large N limit, the saddle points give the dominant contributions, and the saddle point conditions for m_k and \tilde{m}_k are

$$i\tilde{m}_k + \beta p m_k^{p-1} = 0, \quad (24a)$$

$$im_k + \frac{\frac{-i(\beta \gamma - i\tilde{m}_k)}{\sqrt{(\beta \gamma - i\tilde{m}_k)^2 + (\beta \Gamma)^2}} e^{\sum_{k=1}^K \sqrt{(\beta \gamma - i\tilde{m}_k)^2 + (\beta \Gamma)^2}} + \frac{i(\beta \gamma + i\tilde{m}_k)}{\sqrt{(\beta \gamma + i\tilde{m}_k)^2 + (\beta \Gamma)^2}} e^{\sum_{k=1}^K \sqrt{(\beta \gamma + i\tilde{m}_k)^2 + (\beta \Gamma)^2}}}{e^{\sum_{k=1}^K \sqrt{(\beta \gamma - i\tilde{m}_k)^2 + (\beta \Gamma)^2}} + e^{\sum_{k=1}^K \sqrt{(\beta \gamma + i\tilde{m}_k)^2 + (\beta \Gamma)^2}}} = 0. \quad (24b)$$

By eliminating \tilde{m}_k , we obtain

$$m_k + \frac{-\frac{\gamma + p m_k^{p-1}}{\sqrt{(\gamma + p m_k^{p-1})^2 + \Gamma^2}} e^{\sum_{k=1}^K \beta \sqrt{(\gamma + p m_k^{p-1})^2 + \Gamma^2}} + \frac{\gamma - p m_k^{p-1}}{\sqrt{(\gamma - p m_k^{p-1})^2 + \Gamma^2}} e^{\sum_{k=1}^K \beta \sqrt{(\gamma - p m_k^{p-1})^2 + \Gamma^2}}}{e^{\sum_{k=1}^K \beta \sqrt{(\gamma + p m_k^{p-1})^2 + \Gamma^2}} + e^{\sum_{k=1}^K \beta \sqrt{(\gamma - p m_k^{p-1})^2 + \Gamma^2}}} = 0. \quad (25)$$

For large β the condition simplifies to

$$m_k = \frac{\gamma + p|m_k|^{p-1}}{\sqrt{(\gamma + p|m_k|^{p-1})^2 + \Gamma^2}}. \quad (26)$$

For $p = 2$ the function on the RHS of Eq. (26) behaves similarly to $\tanh(\beta m + h)$ appearing in the mean-field theory of the simple Ising model at finite temperature T , where $T = 1/\beta$ is analogous to Γ , and h is analogous to γ .

The free energy F is derived from the partition function via $Z = e^{-\beta N F}$. To calculate F we first use the saddle point result (24a) to write $i\tilde{m}_k = -\beta p m_k^{p-1}$, and then obtain F directly as the saddle point value of the integral in Eq. (23b):

$$F = J(p-1) \sum_{k=1}^K m_k^p - \frac{1}{\beta} \ln \left(e^{\sum_{k=1}^K \beta \sqrt{(\gamma - p m_k^{p-1})^2 + \Gamma^2}} + e^{\sum_{k=1}^K \beta \sqrt{(\gamma + p m_k^{p-1})^2 + \Gamma^2}} \right). \quad (27)$$

In the $\beta \rightarrow \infty$ limit only one of the exponentials in Eq. (27) survives and we obtain:

$$F = J \sum_{k=1}^K \left[(p-1) m_k^p - \sqrt{(\gamma + p|m_k|^{p-1})^2 + \Gamma^2} \right]. \quad (28)$$

To understand how this happens, note that the terms $\pm pm^{p-1}$ in Eq. (27) correspond to the two eigenvalues of σ^z of each penalty qubit. Equation (26) follows from Eq. (25) by dropping the subdominant term with $-p|m|^{p-1}$ in the $T \rightarrow 0$ limit, which is equivalent to having each penalty qubit orient in the same direction. This direction is found as follows. Early in the anneal, when $\Gamma \gg |\gamma \pm pm^{p-1}|$ and the two terms in Eq. (27) are close, the two penalty qubit orientations contribute with nearly equal weights, meaning that thermal noise on the penalty qubits flips their orientations relatively easily even at low temperatures. However, as T is lowered the penalty qubits equilibrate into their minimizing configuration earlier on in the anneal. Once equilibrated, the penalty qubits behave as an effective global field that helps break the symmetry. Eventually, in the $T \rightarrow 0$ limit, this equilibration occurs at the very beginning of the anneal, i.e., at $\Gamma = \infty$. Thus, given enough time to equilibrate, the penalty qubits facilitate the system's evolution toward the ground state.

Stated differently, a sort of simulated annealing works to find the best state of the penalty qubit (classical Ising spin) more efficiently at large Γ than at small Γ . Since the introduction of γ pushes the transition point to large Γ (at finite temperature), we can conclude that the coupling γ is effective at aligning the penalty qubit to the correct orientation.

ADDITIONAL RESULTS FOR THE $p = 2$ CASE

We can solve equation (25) for the Hubbard-Stratonovich field m_k . The solution that minimizes the free energy satisfies $m_k = m$, $\forall k$. We show in Fig. 6 the behavior of m . The second order phase transition occurs at Γ_c when m changes from being zero (the symmetric phase) to being finite (the symmetry-broken phase).

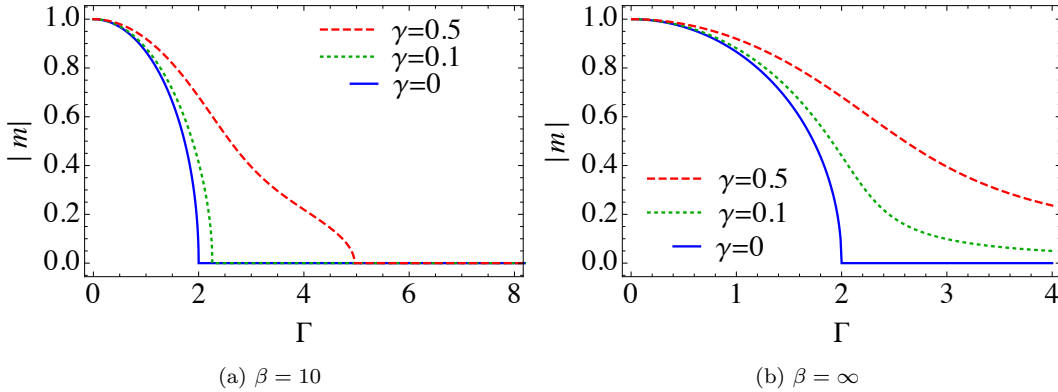


FIG. 6. The solution for $p = 2$ to the saddle-point equation for the Hubbard-Stratonovich field $m_k = m$, $\forall k$ for (a) $\beta = 10$ and (b) $\beta = \infty$. The anneal proceeds from large to small Γ values. At zero temperature, a second order phase transition occurs at $\Gamma = 2$ when $\gamma = 0$, but is pushed to $\Gamma = \infty$ for $\gamma > 0$.

ADDITIONAL RESULTS FOR THE $p > 2$ CASE

As mentioned in the main text, in the zero temperature limit, there exists a single first order transition for $\gamma < \gamma_c$. We show in Fig. 7 the behavior of Γ_c with γ and the dependence of γ_c on p .

In order to illustrate what occurs for the parameter range where two first order phase transitions occur, we show in Fig. 8 a case where for a suitably small temperature sweeping through Γ reveals two phase transitions. In the first transition (Fig. 8(a)), the free energy exhibits two degenerate global minima at $m = 0$ and m_{small} . In the second transition (Fig. 8(b)), the free energy exhibits two degenerate global minima at $m = m_{\text{small}}$ and m_{large} . In various limits, we can recover a single phase transition again. In the limit of $\gamma \rightarrow 0$, m_{small} continuously goes to zero, and the first phase transition vanishes in this limit. As γ increases, m_{small} becomes larger as well and eventually merges with m_{large} , and only a single phase transition occurs. In the zero temperature limit, the minimum at $m = 0$ is absent and there is only a phase transition from m_{small} to m_{large} . The appearance of multiple phase transitions at fixed temperature is generic for $p > 2$, as we show in the phase diagram for multiple p values in Fig. 9.

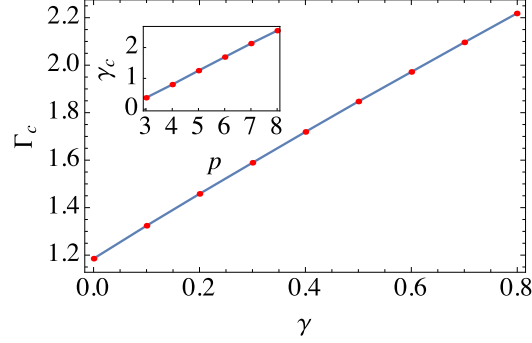


FIG. 7. The critical value Γ_c where the phase transition occurs as a function of γ , for $p = 4$ (dots). The line is a quadratic fit: $\Gamma_c = 1.186 + 1.379\gamma - 0.115\gamma^2$. The phase transition is avoided entirely for $\gamma \gtrsim 0.8$. The inset shows the critical value of γ above which the phase transition disappears for various values of p . The fit is $\gamma_c = -0.99 + 0.46p$.

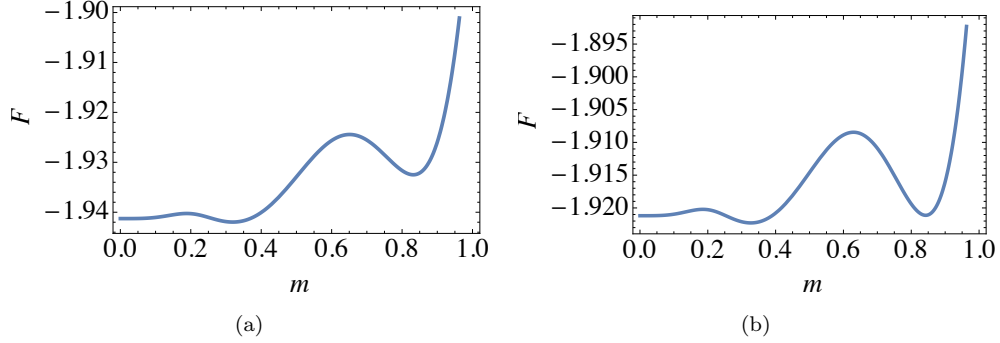


FIG. 8. Free energy as a function of the order parameter m . Parameters are chosen to be $p = 4$, $T = 0.025$, $\gamma = 0.5$ (a) $\Gamma = 1.8698$ (b) $\Gamma = 1.849$. There are three local minima $m = 0$, $m_{\text{small}} \sim 0.3$, and $m_{\text{large}} \sim 0.8$. For large Γ , the quantum fluctuation is large and $m = 0$ is the ground state. As Γ decreases, $F(m_{\text{small}})$ first reaches to the value of $F(m = 0)$, and there is a first order phase transition from $m = 0$ to m_{small} . Then, as Γ further decreases, the free energy $F(m_{\text{large}})$ reaches to $F(m_{\text{small}})$ and another phase transition happens between m_{small} and m_{large} .

NUMERICAL ESTIMATION OF THE SCALING OF THE GAP

Recall the Hamiltonian in the case of uniform ferromagnetic couplings, as defined in Eqs. (4)-(8): $H/J = -\sum_{k=1}^K (H_k^C + \Gamma H_k^D + \gamma H_k^P)$, where $H_k^P = \sum_{i=1}^N \sigma_{ik}^z \sigma_{i0}^z$, $H_k^C = N(S_k^z)^p$, and $H_k^D = \sum_{i=1}^N \sigma_{ik}^x$. At zero temperature and in the absence of a transverse field on the penalty qubits, there is no mechanism for the penalty qubits to flip, so their orientation is fixed by the initial state. This separates the Hilbert space into different sectors, with the sector that has the penalty qubits aligned with the ground state of H_k^C containing the global ground state of H . Let us first consider the case where all penalty qubits point up, i.e., $\sigma_{i0}^z = +1 \forall i$. Note that this decouples the K copies, and the penalty Hamiltonian becomes a global field in the z -direction. The Hamiltonian restricted to this sector can be written as:

$$H^{(0)}/J = \sum_{k=1}^K H_k^{(0)} = -N \sum_{k=1}^K [(S_k^z)^p + \Gamma S_k^x + \gamma S_k^z]. \quad (29)$$

Note that this Hamiltonian is invariant under all permutations of the logical qubit index i . Therefore, if we initialize the system in the symmetric subspace, i.e., if the initial state is symmetric under interchange of logical qubit labels,

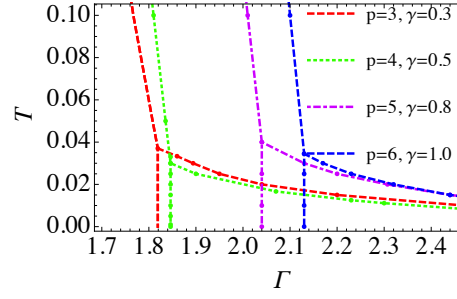


FIG. 9. Phase diagram (Γ, T) for various values of p and γ around $T = 0.04$.

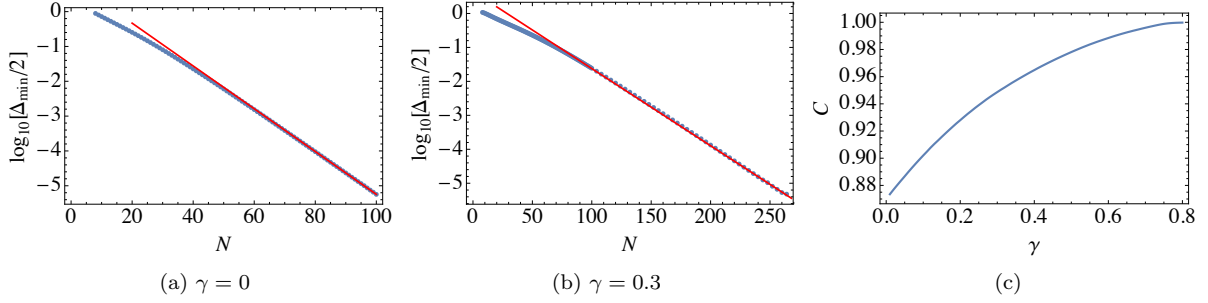


FIG. 10. Behavior of the minimum gap of $H_k^{(0)}$ when restricted to the symmetric subspace, for $p = 4$. For (a), the scaling with N gives $\Delta_{\min} \sim (0.868)^N$ (extracted from the slope of the fit curve (red line)), whereas for (b), the scaling with N gives $\Delta_{\min} \sim (0.949)^N$. (c) The scaling of the gap $\Delta_{\min} \sim C^N$.

the unitary evolution will keep us in this subspace. In the symmetric sector, which is spanned by the Dicke states $\{|J = \frac{N}{2}, M\rangle\}$ with $M = -\frac{N}{2}, \dots, \frac{N}{2}$, the dimensionality of the k th Hamiltonian $H_k^{(0)}$ is reduced from 2^N to $N+1$.^[59] The Dicke states are eigenstates of the collective angular momentum operators

$$s^\alpha = \frac{1}{2} \sum_{i=1}^N \sigma_i^\alpha = \frac{N}{2} S^\alpha, \quad (30)$$

with

$$s^z |J, M_J\rangle = M_J |J, M_J\rangle, \quad s^\pm |J, M_J\rangle = ((J \mp M)(J \pm M + 1))^{1/2} |J, M_J \pm 1\rangle, \quad (31)$$

and $s^\pm = s^x \pm i s^y$ [60]. Thus $\langle J, M_J | s^z | J, M_J \rangle = M_J$ and $\langle J, M_J | s^x | J, M_J \pm 1 \rangle = \frac{1}{2} (J(J+1) - M_J(M_J \pm 1))^{1/2}$, and the only non-vanishing matrix elements of $H_k^{(0)} = -2 \left[\left(\frac{2}{N} \right)^{p-1} (s_k^z)^p + \Gamma s_k^x + \gamma s_k^z \right]$ in the Dicke basis $\{|J = \frac{N}{2}, M\rangle\} \equiv \{|M\rangle\}$ are given by:

$$\langle M | H_k^{(0)} | M \rangle = -2 \left[\left(\frac{2}{N} \right)^{p-1} M^p + \gamma M \right], \quad (32a)$$

$$\langle M | H_k^{(0)} | M \pm 1 \rangle = -\Gamma \left[\frac{N}{2} \left(\frac{N}{2} + 1 \right) - M(M \pm 1) \right]^{1/2}. \quad (32b)$$

The Hamiltonian is thus tridiagonal and can be efficiently diagonalized. Doing so for sufficiently large N 's allows us to extract the scaling of the minimum gap in this sector. The result is shown in Fig. 10.

HOPFIELD MODEL

In this section, we derive the partition function of the Hopfield model, following the method used in Ref. [55]. The Hamiltonian of the Hopfield model is given by [see Eqs. (4)-(9) with $\varepsilon = 0$]:

$$H = -N \sum_{\mu=1}^R \sum_{k=1}^K \left(\frac{1}{N} \sum_{i=1}^N \xi_i^\mu \sigma_{ik}^z \right)^p - \Gamma \sum_{k=1}^K \sum_{i=1}^N \sigma_{ik}^x - \gamma \sum_{k=1}^K \sum_{i=1}^N \sigma_{ik}^z \sigma_{i0}^z. \quad (33)$$

In what follows, we will consistently use the following labels: $k \in [1, K]$ denotes the copy index; $\rho \in [1, n]$ denotes the replica index; $\mu \in [1, R]$ denotes the pattern index; $\alpha \in [1, M]$ denotes the Trotter index.

Let us first consider the case of a finite number of patterns embedded, i.e., $R = \mathcal{O}(N^0)$, and assume that the magnetization is non-zero only for a finite number of μ 's:

$$m_k^\mu = m_k \text{ for } 0 \leq \mu \leq l, \quad m_k^\mu = 0 \text{ for } \mu \geq l+1. \quad (34)$$

In this case, one can take the same steps as in the uniform ferromagnetic case to compute the partition function. Starting from Eq. (19c), including the pattern index and dropping the prime superscript on \tilde{m}_k since it will not matter in the end, we have

$$Z = \prod_{k=1}^K \prod_{\mu=1}^R \int dm_k^\mu \int d\tilde{m}_k^\mu e^{(iN \sum_{\mu} m_k^\mu \tilde{m}_k^\mu + \beta N \sum_{\mu} (m_k^\mu)^p)} \prod_{i=1}^N \left(\text{Tr} \prod_{k=1}^K e^{-i \sum_{\mu} \tilde{m}_k^\mu \xi_i^\mu \sigma_{ik}^z + \beta \gamma \sigma_{ik}^z \sigma_{i0}^z + \beta \Gamma \sigma_{ik}^x} \right). \quad (35)$$

We next trace over the penalty qubit and then use the eigenvalues of the operators in the remaining exponents to perform the trace over the other qubits:

$$\begin{aligned} Z &= \prod_{k=1}^K \prod_{\mu=1}^R \int dm_k^\mu \int d\tilde{m}_k^\mu \exp \left(iN \sum_{\mu} m_k^\mu \tilde{m}_k^\mu + \beta N \sum_{\mu} (m_k^\mu)^p \right. \\ &\quad \left. + \sum_{i=1}^N \log \left(\text{Tr} \prod_k e^{-i \sum_{\mu} \tilde{m}_k^\mu \xi_i^\mu \sigma_{ik}^z + \beta \gamma \sigma_{ik}^z + \beta \Gamma \sigma_{ik}^x} + \text{Tr} \prod_k e^{-i \sum_{\mu} \tilde{m}_k^\mu \xi_i^\mu \sigma_{ik}^z - \beta \gamma \sigma_{ik}^z + \beta \Gamma \sigma_{ik}^x} \right) \right) \end{aligned} \quad (36a)$$

$$\begin{aligned} &= \prod_{k=1}^K \prod_{\mu=1}^R \int dm_k^\mu \int d\tilde{m}_k^\mu \exp \left(iN \sum_{\mu} m_k^\mu \tilde{m}_k^\mu + \beta N \sum_{\mu} (m_k^\mu)^p \right. \\ &\quad \left. + \sum_{i=1}^N \log \left[\prod_k \left(e^{\sqrt{(\beta \gamma - i \sum_{\mu} \tilde{m}_k^\mu \xi_i^\mu)^2 + (\beta \Gamma)^2}} + e^{-\sqrt{(\beta \gamma - i \sum_{\mu} \tilde{m}_k^\mu \xi_i^\mu)^2 + (\beta \Gamma)^2}} \right) \right. \right. \\ &\quad \left. \left. + \prod_k \left(e^{\sqrt{(\beta \gamma + i \sum_{\mu} \tilde{m}_k^\mu \xi_i^\mu)^2 + (\beta \Gamma)^2}} + e^{-\sqrt{(\beta \gamma + i \sum_{\mu} \tilde{m}_k^\mu \xi_i^\mu)^2 + (\beta \Gamma)^2}} \right) \right] \right). \end{aligned} \quad (36b)$$

In the large β limit, only terms that have a positive exponent contribute to the partition function:

$$\begin{aligned} Z &\approx \prod_{k=1}^K \prod_{\mu=1}^R \int dm_k^\mu \int d\tilde{m}_k^\mu \exp \left(iN \sum_{\mu} m_k^\mu \tilde{m}_k^\mu + \beta N \sum_{\mu} (m_k^\mu)^p \right. \\ &\quad \left. + \sum_{i=1}^N \log \left(e^{\sum_k \sqrt{(\beta \gamma - i \sum_{\mu} \tilde{m}_k^\mu \xi_i^\mu)^2 + (\beta \Gamma)^2}} + e^{\sum_k \sqrt{(\beta \gamma + i \sum_{\mu} \tilde{m}_k^\mu \xi_i^\mu)^2 + (\beta \Gamma)^2}} \right) \right). \end{aligned} \quad (37)$$

In the large N limit, the saddle points again give the dominant contributions, and the saddle point condition found from differentiating with respect to m_k^μ is the same as Eq. (24a), i.e., $i\tilde{m}_k^\mu = -\beta p(m_k^\mu)^{p-1}$. The free energy, obtained from $Z = \exp(-\beta N F)$, is therefore similar to Eq. (27):

$$F = J(p-1) \sum_{\mu,k} (m_k^\mu)^p - \frac{1}{\beta N} \sum_{i=1}^N \log \left(e^{\sum_k \beta \sqrt{(\gamma + \sum_{\mu} p(m_k^\mu)^{p-1} \xi_i^\mu)^2 + \Gamma^2}} + e^{\sum_k \beta \sqrt{(\gamma - \sum_{\mu} p(m_k^\mu)^{p-1} \xi_i^\mu)^2 + \Gamma^2}} \right). \quad (38)$$

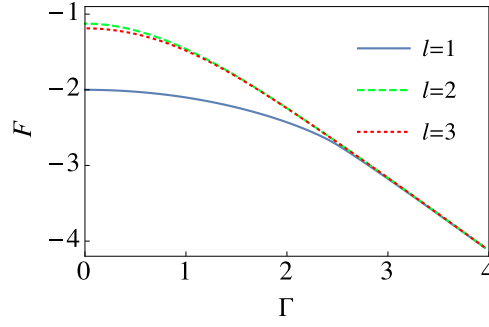


FIG. 11. Hopfield Free energy at $\gamma = 1$ for $l = 1, 2, 3$ red (small dashes), green (large dashes), blue (solid) respectively. $l = 1$ gives the lowest energy.

In the large N limit, the sum over lattice sites i can be replaced by the average of ξ_i^μ , i.e. the self-averaging property,

$$\frac{1}{N} \sum_{i=1}^N f(\xi_i) \xrightarrow{N \rightarrow \infty} [f(\xi)], \quad (39)$$

where $[f(\xi)]$ is the average of $f(\xi)$ over the distribution of ξ . For $l = 1, 2$ and 3 , the results are shown in Fig. 11. The case of $l = 1$ has the lowest free energy, and consequently, all the conclusions of the previous section for the pure ferromagnet apply to the present Hopfield model as well.

HOPFIELD MODEL - MULTI-PATTERN CASE

We next consider the case where the number of embedded patterns R increases with the system size N .

The case of $p \geq 3$

Let us first consider the case of $p \geq 3$. We assume that only a single pattern has a non-vanishing expectation value $m_\alpha^{\mu k} = \mathcal{O}(N^0)$ for $\mu = 1$ and other order parameters take non-zero values from coincidental overlapping $m_\alpha^{\mu k} = \mathcal{O}(N^{-1/2})$ for $\mu \geq 2$. In contrast to the finite pattern case, the contribution of those coincidental overlaps is not negligible if the number of μ increases as a function of the system size N . Below we will often use the following relation,

$$\sum_{1=i_1 < \dots < i_p}^N f(i_1, \dots, i_p) = \frac{1}{p!} \sum_{i_1, \dots, i_p=1}^N f(i_1, \dots, i_p) + \mathcal{O}(N^{p-1}), \quad (40)$$

where $f(i_1, \dots, i_p)$ is a function symmetric under permutation of indices. For convenience of calculations, we temporarily divide the leading interaction part of the Hamiltonian Eq. (33) by $p!$

$$H = -\frac{N}{p!} \sum_{\mu=1}^R \sum_{k=1}^K \left(\frac{1}{N} \sum_{i=1}^N \xi_i^\mu \sigma_{ik}^z \right)^p - \Gamma \sum_{k=1}^K \sum_{i=1}^N \sigma_{ik}^x - \gamma \sum_{k=1}^K \sum_{i=1}^N \sigma_{ik}^z \sigma_{iz}^0. \quad (41)$$

The original Eq. (33) without $p!$ will be recovered at the end of computations.

The partition function is, up to a trivial factor involving a power of 2π ,

$$Z = \sum_{\sigma} \prod_{\mu, \alpha, k} \int dm_{k\alpha}^\mu d\tilde{m}_{k\alpha}^\mu (\prod \langle \sigma | \sigma \rangle) \exp \left(i \frac{\beta}{M} \tilde{m}_{k\alpha}^1 (N m_{k\alpha}^1 - \sum_i \xi_i^1 \sigma_{ik}^z(\alpha)) + \frac{\beta N}{M p!} (m_{k\alpha}^1)^p + \frac{\beta N}{M} \sum_{\mu=2}^R \frac{1}{N^p} \sum_{i_1 < \dots < i_p} \xi_{i_1}^\mu \dots \xi_{i_p}^\mu \sigma_{i_1 k}^z(\alpha) \dots \sigma_{i_p k}^z(\alpha) \right)$$

$$+\frac{\beta\Gamma}{M}\sum_i\sigma_{ik}^x(\alpha)+\frac{\beta\gamma}{M}\sum_i\sigma_{ik}^z(\alpha)\sigma_{i0}^z(\alpha)\Big), \quad (42)$$

where we used a simplified notation

$$\prod\langle\sigma|\sigma\rangle\equiv\langle\sigma_{i0}^z(\alpha)|\sigma_{i0}^x(\alpha)\rangle\langle\sigma_{i0}^x(\alpha)|\sigma_{i0}^z(\alpha+1)\rangle\prod_{k=1}^K\langle\sigma_{ik}^z(\alpha)|\sigma_{ik}^x(\alpha)\rangle\langle\sigma_{ik}^x(\alpha)|\sigma_{ik}^z(\alpha+1)\rangle. \quad (43)$$

We use the replica method to evaluate the configurational average of the free energy [61],

$$[\ln Z]=\lim_{n\rightarrow 0}\frac{[Z^n]-1}{n}, \quad (44)$$

where the square brackets denote the average over the distribution of random patterns ξ_i^μ . Let us denote the replica index as $\rho = 1, 2, \dots, n$. All the variables are replicated, for instance, as $m_\alpha^{\mu k} \rightarrow m_\rho^{\mu k}(\alpha)$. The replicated partition function is ,

$$\begin{aligned} Z^n = & \sum_\sigma \prod_{\mu, \alpha, k, \rho} \int dm_\rho^{\mu k}(\alpha) d\tilde{m}_\rho^{\mu k}(\alpha) (\prod \langle \sigma | \sigma \rangle) \exp \left(i \frac{\beta}{M} \sum_{\alpha, k, \rho} \tilde{m}_\rho^{1k}(\alpha) (Nm_\rho^{1k}(\alpha) - \sum_i \xi_i^1 \sigma_{i\rho z}^k(\alpha)) + \frac{\beta N}{Mp!} (m_\rho^{1k}(\alpha))^p + \right. \\ & + \sum_{\mu \geq 2} \sum_{\alpha k \rho} \frac{\beta}{MN^{p-1}} \sum_{i_1 < i_2 < \dots < i_p} \xi_{i_1}^\mu \dots \xi_{i_p}^\mu \sigma_{i_1 \rho z}^k(\alpha) \dots \sigma_{i_p \rho z}^k(\alpha) \\ & \left. + \frac{\beta\Gamma}{M} \sum_i \sum_{\alpha, k, \rho} \sigma_{i\rho x}^k(\alpha) + \frac{\beta\gamma}{M} \sum_i \sum_{\alpha, k, \rho} \sigma_{i\rho z}^k(\alpha) \sigma_{i\rho z}^0(\alpha) \right). \end{aligned} \quad (45)$$

To take the configurational average over $\xi_i^\mu = \pm 1$ ($\mu \geq 2$), we evaluate the cummulants of the term involving $\xi_{i_1}^\mu \dots \xi_{i_p}^\mu$. The term linear in ξ vanishes by symmetry. The next quadratic term involving

$$\sum_{i_1 < \dots < i_p} \sum_{i'_1 < \dots < i'_p} \left[\xi_{i_1}^\mu \dots \xi_{i_p}^\mu \xi_{i'_1}^\mu \dots \xi_{i'_p}^\mu \right] \quad (46)$$

survives only when $i_1 = i'_1, \dots, i_p = i'_p$. Thus we find for the quadratic term

$$\begin{aligned} & \frac{1}{2} \left(\frac{\beta}{MN^{p-1}} \right)^2 \sum_{\substack{\alpha k \rho, \alpha' k' \rho', \\ i_1 < i_2 < \dots < i_p}} \sigma_{i_1 \rho z}^k(\alpha) \sigma_{i_1 \rho' z}^{k'}(\alpha') \dots \sigma_{i_p \rho z}^k(\alpha) \sigma_{i_p \rho' z}^{k'}(\alpha') \\ & = \frac{1}{2} \left(\frac{\beta}{MN^{p-1}} \right)^2 \sum_{\alpha k \rho, \alpha' k' \rho'} \frac{1}{p!} \left(\sum_i \sigma_{i \rho z}^k(\alpha) \sigma_{i \rho' z}^{k'}(\alpha') \right)^p \\ & = \frac{1}{2p!} \left(\frac{\beta}{M} \right)^2 \sum_{\alpha k \rho, \alpha' k' \rho'} \frac{1}{N^{p-2}} \left(\frac{1}{N} \sum_i \sigma_{i \rho z}^k(\alpha) \sigma_{i \rho' z}^{k'}(\alpha') \right)^p. \end{aligned} \quad (47)$$

The leading term of the cubic cumulant is proportional to

$$\frac{1}{(N^{p-1})^3} \left[\left(\sum_{i_1 < \dots < i_p} \xi_{i_1}^\mu \dots \xi_{i_p}^\mu \sigma_{i_1 \rho z}^k(\alpha) \dots \sigma_{i_p \rho z}^k(\alpha) \right)^3 \right]. \quad (48)$$

The sum $\sum_i \xi_i^\mu \sigma_{i \rho z}^k(\alpha)$ is $\mathcal{O}(N^{1/2})$ due to coincidental overlap, and hence the above expression is $\mathcal{O}(N^{3p/2}/N^{3p-3})$. For $p \geq 3$, this can be neglected in the limit $N \rightarrow \infty$ compared to the leading term of $\mathcal{O}(N)$. The same applies to higher-order cumulants. Therefore the total contribution from $\mu \geq 2$ is

$$\prod_{\mu \geq 2}^R \exp \left(\frac{1}{2p!} \left(\frac{\beta}{M} \right)^2 \frac{1}{N^{p-2}} \sum_{\alpha k \rho, \alpha' k' \rho'} \left(\frac{1}{N} \sum_i \sigma_{i \rho z}^k(\alpha) \sigma_{i \rho' z}^{k'}(\alpha') \right)^p \right)$$

$$= \exp \left(\frac{aN}{2p!} \left(\frac{\beta}{M} \right)^2 \sum_{\alpha k \rho, \alpha' k' \rho'} \left(\frac{1}{N} \sum_i \sigma_{i\rho z}^k(\alpha) \sigma_{i\rho' z}^{k'}(\alpha') \right)^p \right), \quad (49)$$

where we defined $a = R/N^{p-1}$. Then the total partition function is

$$\begin{aligned} [Z^n] &= \sum_{\sigma} \prod_{\mu \alpha k \rho} \int dm_{\rho}^{\mu k}(\alpha) d\tilde{m}_{\rho}^{\mu k}(\alpha) \prod \langle \sigma | \sigma \rangle \\ &\exp \left(\sum_{\alpha k \rho} \frac{\beta N}{M p!} (m_{\rho}^{1k}(\alpha))^p + i \frac{\beta N}{M} \sum_{\alpha k \rho} \tilde{m}_{\rho}^{1k}(\alpha) m_{\rho}^{1k}(\alpha) + \frac{aN}{2p!} \left(\frac{\beta}{M} \right)^2 \sum_{\alpha k \rho, \alpha' k' \rho'} \left(\frac{1}{N} \sum_i \sigma_{i\rho z}^k(\alpha) \sigma_{i\rho' z}^{k'}(\alpha') \right)^p \right. \\ &\left. - i \frac{\beta}{M} \sum_{\alpha k \rho} \tilde{m}_{\rho}^{1k}(\alpha) \sum_i \xi_i^1 \sigma_{i\rho z}^k(\alpha) + \frac{\beta \Gamma}{M} \sum_i \sum_{\alpha k \rho} \sigma_{i\rho x}^k(\alpha) + \frac{\beta \gamma}{M} \sum_i \sum_{\alpha k \rho} \sigma_{i\rho z}^k \sigma_{i\rho z}^0(\alpha) \right). \end{aligned} \quad (50)$$

We linearize the term involving the p th power of spin variables in the above equation by introducing auxiliary fields $q_{\rho\rho'}^{kk'}(\alpha, \alpha')$ and $\tilde{q}_{\rho\rho'}^{kk'}(\alpha, \alpha')$ for $\rho \neq \rho'$ and $R_{\rho}^{kk'}(\alpha, \alpha')$ and $\tilde{R}_{\rho}^{kk'}(\alpha, \alpha')$ for $\rho = \rho'$,

$$\begin{aligned} [Z^n] &= \sum_{\sigma} \prod_{\mu \alpha k \rho} \int dm_{\rho}^{\mu k}(\alpha) d\tilde{m}_{\rho}^{\mu k}(\alpha) \prod \langle \sigma | \sigma \rangle \exp \left(\sum_{\alpha k \rho} \frac{\beta N}{M p!} (m_{\rho}^{1k}(\alpha))^p + i \frac{\beta N}{M} \sum_{\alpha k \rho} \tilde{m}_{\rho}^{1k}(\alpha) m_{\rho}^{1k}(\alpha) \right. \\ &+ \frac{aN}{2p!} \left(\frac{\beta}{M} \right)^2 \sum_{\substack{kk' \alpha \alpha' \\ \rho \neq \rho'}} (q_{\rho\rho'}^{kk'}(\alpha, \alpha'))^p + \frac{aN}{2p!} \left(\frac{\beta}{M} \right)^2 \sum_{\substack{kk' \alpha \alpha' \\ \rho}} (R_{\rho}^{kk'}(\alpha, \alpha'))^p \\ &+ i \frac{a\beta^2}{2M^2} \sum_{\substack{kk' \alpha \alpha' \\ \rho \neq \rho'}} \tilde{q}_{\rho\rho'}^{kk'}(\alpha, \alpha') \left(N q_{\rho\rho'}^{kk'}(\alpha, \alpha') - \sum_i \sigma_{i\rho z}^k(\alpha) \sigma_{i\rho' z}^{k'}(\alpha') \right) \\ &+ i \frac{a\beta^2}{2M^2} \sum_{\substack{kk' \alpha \alpha' \\ \rho}} \tilde{R}_{\rho}^{kk'}(\alpha, \alpha') \left(N R_{\rho}^{kk'}(\alpha, \alpha') - \sum_i \sigma_{i\rho z}^k(\alpha) \sigma_{i\rho z}^{k'}(\alpha') \right) \\ &\left. - i \frac{\beta}{M} \sum_{\alpha k \rho} \tilde{m}_{\rho}^{1k}(\alpha) \sum_i \xi_i^1 \sigma_{i\rho z}^k(\alpha) + \frac{\beta \Gamma}{M} \sum_i \sum_{\alpha k \rho} \sigma_{i\rho x}^k(\alpha) + \frac{\beta \gamma}{M} \sum_i \sum_{\alpha k \rho} \sigma_{i\rho z}^k \sigma_{i\rho z}^0(\alpha) \right). \end{aligned} \quad (51)$$

We use the replica-symmetric ansatz as well as the static approximation and consider only the saddle point solution,

$$m_{\rho}^{1k}(\alpha) = m, \quad \tilde{m}_{\rho}^{1k}(\alpha) = i\tilde{m}, \quad \xi_i^1 = \xi, \quad q_{\rho\rho'}^{kk'}(\alpha, \alpha') = q, \quad \tilde{q}_{\rho\rho'}^{kk'}(\alpha, \alpha') = i\tilde{q}, \quad R_{\rho}^{kk'}(\alpha, \alpha') = i\tilde{R}. \quad (52)$$

The spin-dependent part Z' of Eq. (51) is quadratic in spin variables. One can linearize it by introducing auxiliary parameters z and w for Gaussian integrations. For fixed site index i , we find

$$\begin{aligned} Z' &= \sum_{\sigma} \prod \langle \sigma | \sigma \rangle \exp \left(\frac{\beta}{M} \sum_{\alpha k \rho} \tilde{m} \sigma_{\rho z}^k(\alpha) \xi + \frac{\beta \Gamma}{M} \sum_{\alpha k \rho} \sigma_{\rho x}^k(\alpha) + \frac{\beta \gamma}{M} \sum_{\alpha k \rho} \sigma_{\rho z}^k(\alpha) \sigma_{\rho z}^0(\alpha) \right. \\ &\left. + \frac{a}{2} \left(\frac{\beta}{M} \right)^2 \sum_{\substack{kk' \alpha \alpha' \\ \rho \neq \rho'}} \tilde{q} \sigma_{\rho z}^k(\alpha) \sigma_{\rho' z}^{k'}(\alpha') + \frac{a}{2} \left(\frac{\beta}{M} \right)^2 \sum_{\substack{kk' \alpha \alpha' \\ \rho}} (\tilde{R} - \tilde{q}) \sigma_{\rho z}^k(\alpha) \sigma_{\rho z}^{k'}(\alpha') \right) \end{aligned} \quad (53a)$$

$$\begin{aligned} &= \sum_{\sigma} \prod \langle \sigma | \sigma \rangle \int Dz \exp \left(\frac{z\beta}{M} \sqrt{a\tilde{q}} \sum_{\alpha k \rho} \sigma_{\rho z}^k(\alpha) \right) \exp \left(\frac{a}{2} \left(\frac{\beta}{M} \right)^2 \sum_{\alpha \alpha' k k' \rho} (\tilde{R} - \tilde{q}) \sigma_{\rho z}^k(\alpha) \sigma_{\rho z}^{k'}(\alpha') \right) \\ &\exp \left(\frac{\beta}{M} \tilde{m} \sum_{\alpha k \rho} \xi \sigma_{\rho z}^k(\alpha) + \frac{\beta \Gamma}{M} \sum_{\alpha k \rho} \sigma_{\rho x}^k(\alpha) + \frac{\beta \gamma}{M} \sum_{\alpha k \rho} \sigma_{\rho z}^k(\alpha) \sigma_{\rho z}^0(\alpha) \right), \end{aligned} \quad (53b)$$

where Dz is the Gaussian measure $Dz = dz \exp(-z^2/2)/\sqrt{2\pi}$. Now the summation over spin variable can be carried out independently for each ρ , which gives an expression of the form $\int Dz(\dots)^n$. We further linearize the term involving

$\tilde{R} - \tilde{q}$ by a Gaussian integral to find

$$\int Dz \left\{ \sum_{\sigma} \prod \langle \sigma | \sigma \rangle \exp \left(\frac{z\beta}{M} \sqrt{a\tilde{q}} \sum_{\alpha k} \sigma_z^k(\alpha) \right) \int Dw \exp \left(\frac{w\beta}{M} \sqrt{a(\tilde{R} - \tilde{q})} \sum_{\alpha k} \sigma_z^k(\alpha) \right) \right. \\ \left. \exp \left(\frac{\beta}{M} \tilde{m} \sum_{\alpha k} \xi \sigma_z^k(\alpha) + \frac{\beta\Gamma}{M} \sum_{\alpha k} \sigma_x^k(\alpha) + \frac{\beta\gamma}{M} \sum_{\alpha k} \sigma_z^k(\alpha) \sigma_z^0(\alpha) \right) \right\}^n, \quad (54)$$

To take the $n \rightarrow 0$ limit according to the replica method Eq. (44), we evaluate the linear in n term in the expansion of the above equation,

$$n \int Dz \ln \sum_{\sigma} \int Dw \prod_{\alpha k} \exp \left(\frac{\beta}{M} \left(\sqrt{a\tilde{q}} z + \sqrt{a(\tilde{R} - \tilde{q})} w \right) \sigma_z^k(\alpha) \right) \\ \exp \left(\frac{\beta}{M} \left(\tilde{m} \xi \sigma_z^k(\alpha) + \gamma \sigma_z^k(\alpha) \sigma_z^0(\alpha) + \Gamma \sigma_x^k(\alpha) \right) \right) \prod \langle \sigma | \sigma \rangle. \quad (55)$$

In the limit $M \rightarrow \infty$, the trace can be evaluated as

$$n \int Dz \ln \int Dw \left(\left[2 \cosh \beta \sqrt{\left(\tilde{m} \xi + \gamma + \sqrt{a\tilde{q}} z + \sqrt{a(\tilde{R} - \tilde{q})} w \right)^2 + \Gamma^2} \right]^K + \right. \\ \left. \left[2 \cosh \beta \sqrt{\left(\tilde{m} \xi - \gamma + \sqrt{a\tilde{q}} z + \sqrt{a(\tilde{R} - \tilde{q})} w \right)^2 + \Gamma^2} \right]^K \right). \quad (56)$$

At this stage, we need to take the average over $\xi = \pm 1$. One can see that the spin part becomes a sum of four terms: $\cosh \beta \sqrt{\pm \tilde{m} \pm \gamma + \dots}$. However, two of them are identical by the reflection $z(w) \rightarrow -z(-w)$. Therefore, one can just insert $\xi = 1$ in the above expression. The final form of the partition function is

$$Z = \exp \left\{ \beta N K n m^p - \beta N K n \tilde{m} m + \frac{aN}{2} \beta^2 K^2 n(n-1) q^p + \frac{aN}{2} \beta^2 K^2 n R^p \right. \\ \left. - \frac{a\beta^2}{2} N K^2 n(n-1) \tilde{q} q - \frac{a\beta^2}{2} N K^2 n \tilde{R} R + nN \int Dz \ln \int Dw \left((2 \cosh \beta u_+)^K + (2 \cosh \beta K u_-)^K \right) \right\}, \quad (57)$$

where

$$u_{\pm} = \sqrt{\left(\tilde{m} \pm \gamma + \sqrt{a\tilde{q}} z + \sqrt{a(\tilde{R} - \tilde{q})} w \right)^2 + \Gamma^2}. \quad (58)$$

We have dropped the factor $1/p!$ in front of m^p , q^p , and R^p to recover the original form of the Hamiltonian (33) from Eq. (41). The free energy F defined by $Z = \exp(-N\beta nF)$ is given by

$$F/(JK) = -m^p + \tilde{m} m + \frac{a\beta K}{2} q^p - \frac{a\beta K}{2} R^p - \frac{a\beta K}{2} \tilde{q} q + \frac{a\beta K}{2} \tilde{R} R \\ - \frac{1}{\beta K} \int Dz \ln \int Dw \left((2 \cosh \beta u_+)^K + (2 \cosh \beta u_-)^K \right). \quad (59)$$

The consistency conditions for m, q, R and $\tilde{m}, \tilde{q}, \tilde{R}$ are

$$\tilde{m} = pm^{p-1}, \quad (60a)$$

$$\tilde{q} = pq^{p-1}, \quad (60b)$$

$$\tilde{R} = pR^{p-1}, \quad (60c)$$

$$m = \int Dz Y^{-1} \int Dw \left(\frac{g_+}{u_+} (2 \cosh \beta u_+)^{K-1} (2 \sinh \beta u_+) + \frac{g_-}{u_-} (2 \cosh \beta u_-)^{K-1} (2 \sinh \beta u_-) \right), \quad (60d)$$

$$q = \int Dz Y^{-2} \int Dw \left[\left(\frac{g_+}{u_+} (2 \cosh \beta u_+)^{K-1} (2 \sinh \beta u_+) \right)^2 + \left(\frac{g_-}{u_-} (2 \cosh \beta u_-)^{K-1} (2 \sinh \beta u_-) \right)^2 \right], \quad (60e)$$

$$\begin{aligned} R = \frac{1}{\beta K} \int Dz Y^{-1} \int Dw & \left[\beta (K-1) (2 \cosh \beta u_+)^{K-2} (2 \sinh \beta u_+)^2 \left(\frac{g_+}{u_+} \right)^2 + \beta (2 \cosh \beta u_+)^K \left(\frac{g_+}{u_+} \right)^2 \right. \\ & + (2 \cosh \beta u_+)^{K-2} (2 \sinh \beta u_+)^2 \frac{\Gamma^2}{u_+^3} + \beta (K-1) (2 \cosh \beta u_-)^{K-2} (2 \sinh \beta u_-)^2 \left(\frac{g_-}{u_-} \right)^2 \\ & \left. + \beta (2 \cosh \beta u_-)^K \left(\frac{g_-}{u_-} \right)^2 + (2 \cosh \beta u_-)^{K-2} (2 \sinh \beta u_-)^2 \frac{\Gamma^2}{u_-^3} \right], \end{aligned} \quad (60f)$$

where

$$g_{\pm} = \left(\tilde{m} \pm \gamma + \sqrt{a\tilde{q}}z + \sqrt{a(\tilde{R} - \tilde{q})}w \right), \quad (61a)$$

$$u_{\pm} = \sqrt{g_{\pm}^2 + \Gamma^2}, \quad (61b)$$

$$Y = \int Dw \left((2 \cosh \beta u_+)^K + (2 \cosh \beta u_-)^K \right). \quad (61c)$$

Inspection of Eqs. (60e) and (60f) reveals that R approaches q in the low temperature limit. Consequently, $\tilde{R} - \tilde{q}$ goes to zero, and the w dependence in the integrands disappears. We therefore have, for $\beta \gg 1$,

$$m = \int Dz Y^{-1} \left(\frac{g_+}{u_+} (2 \cosh \beta u_+)^{K-1} (2 \sinh \beta u_+) + \frac{g_-}{u_-} (2 \cosh \beta u_-)^{K-1} (2 \sinh \beta u_-) \right), \quad (62a)$$

$$q = \int Dz Y^{-2} \left[\left(\frac{g_+}{u_+} (2 \cosh \beta u_+)^{K-1} (2 \sinh \beta u_+) \right)^2 + \left(\frac{g_-}{u_-} (2 \cosh \beta u_-)^{K-1} (2 \sinh \beta u_-) \right)^2 \right], \quad (62b)$$

$$\begin{aligned} R = \frac{1}{\beta K} \int Dz Y^{-1} & \left[\beta (K-1) (2 \cosh \beta u_+)^{K-2} (2 \sinh \beta u_+)^2 \left(\frac{g_+}{u_+} \right)^2 + \beta (2 \cosh \beta u_+)^K \left(\frac{g_+}{u_+} \right)^2 \right. \\ & + (2 \cosh \beta u_+)^{K-2} (2 \sinh \beta u_+)^2 \frac{\Gamma^2}{u_+^3} + \beta (K-1) (2 \cosh \beta u_-)^{K-2} (2 \sinh \beta u_-)^2 \left(\frac{g_-}{u_-} \right)^2 \\ & \left. + \beta (2 \cosh \beta u_-)^K \left(\frac{g_-}{u_-} \right)^2 + (2 \cosh \beta u_-)^{K-2} (2 \sinh \beta u_-)^2 \frac{\Gamma^2}{u_-^3} \right]. \end{aligned} \quad (62c)$$

Without loss of generality, we can restrict the parameter region to $\tilde{m} \geq 0$ and $\gamma \geq 0$. Then, in the limit $\beta \rightarrow \infty$,

$\beta u_+ \gg \beta u_-$, and thus

$$m = \int Dz Y^{-1} \left(\frac{g_+}{u_+} (2 \cosh \beta u_+)^{K-1} (2 \sinh \beta u_+) \right) \rightarrow \int Dz \frac{g_+}{u_+} , \quad (63a)$$

$$q = \int Dz Y^{-2} \left[\left(\frac{g_+}{u_+} (2 \cosh \beta u_+)^{K-1} (2 \sinh \beta u_+) \right)^2 \right] \rightarrow \int Dz \frac{g_+^2}{u_+^2} , \quad (63b)$$

$$R = \frac{1}{\beta K} \int Dz Y^{-1} \left[\beta (K-1) (2 \cosh \beta u_+)^{K-2} (2 \sinh \beta u_+)^2 \left(\frac{g_+}{u_+} \right)^2 + \beta (2 \cosh \beta u_+)^K \left(\frac{g_+}{u_+} \right)^2 + (2 \cosh \beta u_+)^{K-2} (2 \sinh \beta u_+)^2 \frac{\Gamma^2}{u_+^3} \right] \rightarrow \int Dz \frac{g_+^2}{u_+^2} , \quad (63c)$$

where

$$g_+ = \left(\tilde{m} + \gamma + \sqrt{a \tilde{q} z} \right) = (pm^{p-1} + \gamma + \sqrt{apq^{p-1}z}) , \quad (64a)$$

$$u_+ = \sqrt{g_+^2 + \Gamma^2} , \quad (64b)$$

$$Y = (2 \cosh \beta u_+)^K . \quad (64c)$$

We show an example of solutions in Fig. 12. The free energy is

$$F/(JK) = (p-1)m^p + \frac{ap(p-1)}{2} C q^{p-1} - \int Dz \sqrt{(pm^{p-1} + \gamma + \sqrt{apq^{p-1}z})^2 + \Gamma^2} , \quad (65)$$

where

$$\lim_{\beta \rightarrow \infty} \beta K(R - q) = \int Dz \frac{\Gamma^2}{u_+^3} \equiv C . \quad (66)$$

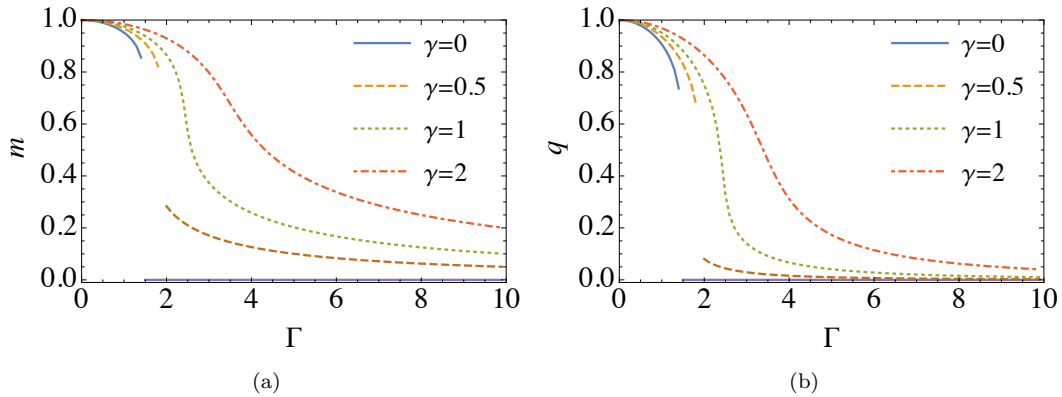


FIG. 12. Behavior of m (a) and q (b) for the Hopfield model with many patterns embedded with $p = 4$, $R = 0.25N^3$ and $K = 3$.

$p = 2$ Case

In this subsection, we use the following convention

$$H/J = -\frac{N}{2} \sum_{\mu=1}^R \sum_{k=1}^K \left(\frac{1}{N} \sum_{i=1}^N \xi_i^\mu \sigma_{ik}^z \right)^2 - \Gamma \sum_k \sum_i \sigma_{ik}^x - \gamma \sum_k \sum_i \sigma_{ik}^z \sigma_{iz}^0 . \quad (67)$$

The replicated partition function is

$$Z^n = \sum_{\sigma} \prod_{\mu \sigma \rho k} \int dm_{\mu\rho}^k(\alpha) \prod \langle \sigma | \sigma \rangle \exp \left(-\frac{\beta N}{2M} \sum_{\alpha \mu \rho k} (m_{\mu\rho}^k(\alpha))^2 + \frac{\beta}{M} \sum_{\alpha \mu \rho k} m_{\mu\rho}^k(\alpha) \xi_i^\mu \sigma_{i\rho z}^k(\alpha) \right) \\ \times \exp \left(\frac{\beta \Gamma}{M} \sum_{\alpha \rho k} \sigma_{i\rho x}^k(\alpha) + \frac{\beta \gamma}{M} \sum_{\alpha \rho k} \sigma_{i\rho z}^k(\alpha) \sigma_{i\rho z}^0(\alpha) \right). \quad (68)$$

We separate the part of $\mu = 1$ from $\mu \geq 2$ as in the case of $p \geq 3$. For $\mu \geq 2$, we keep only the quadratic term of the cumulant expansion of the expectation value $[Z^n]$ under the expectation that $m_{\mu\rho}^k$ is $\mathcal{O}(N^{-1/2})$,

$$\prod_{\mu \geq 2} \exp \left(\frac{\beta}{M} \sum_{\alpha \rho k} m_{\mu\rho}^k(\alpha) \xi_i^\mu \sigma_{i\rho z}^k(\alpha) \right) \simeq \prod_{\mu \geq 2} \exp \left(\frac{\beta^2}{2M^2} \sum_i \sum_{\alpha \alpha' \rho \rho' k k'} m_{\mu\rho}^k(\alpha) m_{\mu\rho'}^{k'}(\alpha') \sigma_{i\rho z}^k(\alpha) \sigma_{i\rho' z}^{k'}(\alpha') \right). \quad (69)$$

We can thus write for $\mu \geq 2$

$$\exp \left(-\frac{\beta N}{2M} \sum_{\alpha, \mu \geq 2, \rho k} (m_{\mu\rho}^k(\alpha))^2 + \frac{\beta}{M} \sum_{\alpha, \mu \geq 2, \rho k} m_{\mu\rho}^k(\alpha) \xi_i^\mu \sigma_{i\rho z}^k(\alpha) \right) \\ \simeq \prod_{\mu \geq 2} \exp \left(-\frac{\beta N}{2M} \sum_{\alpha \alpha' \rho \rho' k k'} \tilde{\Lambda}_{\alpha' \rho' k'}^{\alpha \rho k} m_{\mu\rho}^k(\alpha) m_{\mu\rho'}^{k'}(\alpha') \right), \quad (70)$$

where

$$\tilde{\Lambda}_{\alpha' \rho' k'}^{\alpha \rho k} = \delta_{\alpha' \rho' k'}^{\alpha \rho k} - \frac{\beta}{MN} \sum_i \sigma_{i\rho z}^k(\alpha) \sigma_{i\rho' z}^{k'}(\alpha'). \quad (71)$$

Integrating over $m_{\mu\rho}^k(\alpha)$, we obtain

$$(\det \tilde{\Lambda})^{-(R-1)/2} \simeq (\det \tilde{\Lambda})^{-aN/2} = \exp \left(-\frac{aN}{2} \sum_{\lambda} \ln \lambda \right), \quad (72)$$

where λ are the eigenvalues of $\tilde{\Lambda}$. We linearize the spin dependent terms by introducing auxiliary fields $q_{\rho\rho'}^{kk'}(\alpha, \alpha')$, $\tilde{q}_{\rho\rho'}^{kk'}(\alpha, \alpha')$, $R_{\rho}^{kk'}(\alpha, \alpha')$ and $\tilde{R}_{\rho}^{kk'}(\alpha, \alpha')$ as before. With these auxiliary fields, the matrix elements are

$$\tilde{\Lambda}_{\alpha' \rho' k'}^{\alpha \rho k} = \delta_{\alpha' \rho' k'}^{\alpha \rho k} - \frac{\beta}{M} q_{\rho\rho'}^{kk'}(\alpha, \alpha') - \delta_{\rho\rho'} \frac{\beta}{M} R_{\rho}^{kk'}(\alpha, \alpha'), \quad (73)$$

The integrand in Eq. (68) becomes

$$\exp \left(-\frac{\beta N}{2M} \sum_{\alpha \rho k} (m_{1\rho}^k(\alpha))^2 - \frac{aN}{2} \sum_{\lambda} \ln \lambda - \frac{Na\beta^2}{2M^2} \sum_{\substack{\alpha \alpha' k k' \\ \rho \neq \rho'}} \tilde{q}_{\rho\rho'}^{kk'}(\alpha, \alpha') q_{\rho\rho'}^{kk'}(\alpha, \alpha') \right. \\ \left. - \frac{Na\beta^2}{2M^2} \sum_{\substack{\alpha \alpha' k k' \\ \rho}} \tilde{R}_{\rho}^{kk'}(\alpha, \alpha') R_{\rho}^{kk'}(\alpha, \alpha') \right) \\ \text{Tr} \exp \left(\frac{\beta}{M} \sum_{\alpha \rho k} m_{1\rho}^k(\alpha) \xi_i^1 \sigma_{i\rho z}^k(\alpha) + \frac{a\beta^2}{2M^2} \sum_{\substack{\alpha \alpha' k k' \\ \rho \neq \rho'}} \sum_i \tilde{q}_{\rho\rho'}^{kk'}(\alpha, \alpha') \sigma_{i\rho z}^k(\alpha) \sigma_{i\rho' z}^{k'}(\alpha') \right. \\ \left. + \frac{a\beta^2}{2M^2} \sum_{\substack{\alpha \alpha' k k' \\ \rho}} \sum_i \tilde{R}_{\rho}^{kk'}(\alpha, \alpha') \sigma_{i\rho z}^k(\alpha) \sigma_{i\rho z}^{k'}(\alpha') + \frac{\beta \Gamma}{M} \sum_{\alpha \rho k} \sigma_{i\rho x}^k(\alpha) + \frac{\beta \gamma}{M} \sum_{\alpha \rho k} \sigma_{i\rho z}^k(\alpha) \sigma_{i\rho z}^0(\alpha) \right). \quad (74)$$

Under the replica symmetric and static approximations, the spin dependent part in Eq. (74) has almost the same form as in Eq. (51) and therefore can be evaluated similarly. The result is

$$n \int Dz \ln \text{Tr} \int Dw ((2 \cosh \beta u_+)^K + (2 \cosh \beta u_-)^K) , \quad (75)$$

where

$$u_{\pm} = \sqrt{\left(m \pm \gamma + \sqrt{a\tilde{q}}z + \sqrt{a(\tilde{R} - \tilde{q})}w\right)^2 + \Gamma^2} . \quad (76)$$

Let us use the static and replica symmetric ansatz also for the matrix $\tilde{\Lambda}$,

$$\tilde{\Lambda}_{\alpha', \rho', k'}^{\alpha, \rho, k} = \begin{cases} -\frac{\beta}{M}q & \text{for } \rho \neq \rho' \\ -\frac{\beta}{M}R & \text{for } \rho = \rho' \text{ and } \alpha \neq \alpha' \\ (1 - \frac{\beta}{M}) & \text{for } \rho = \rho' \text{ and } \alpha = \alpha' \text{ and } k = k' \\ -\frac{\beta}{M} & \text{for } \rho = \rho' \text{ and } \alpha = \alpha' \text{ and } k \neq k' \end{cases} , \quad (77)$$

where we used $R_{\rho}^{k k'}(\alpha, \alpha') = R$ for $\alpha \neq \alpha'$ and 1 for $\alpha = \alpha'$. The eigenvalues of $\Lambda_{\alpha', \rho', k'}^{\alpha, \rho, k}$ and their degeneracies are given by

Eigenvalue	degeneracy
1	$n(M(K-1))$
$1 - K\frac{\beta}{M} + K\frac{\beta}{M}R$	$n(M-1)$
$1 - K\frac{\beta}{M} - K(M-1)\frac{\beta}{M}R + KM\frac{\beta}{M}q$	$(n-1)$
$1 - K\frac{\beta}{M} - K(M-1)\frac{\beta}{M}R - K(n-1)M\frac{\beta}{M}q$	1

(78)

Thus, for $M \rightarrow \infty$ and $n \rightarrow 0$,

$$\sum_{\lambda} \ln \lambda = n \left(\ln(1 - K\beta R + K\beta q) - \frac{K\beta q}{1 - K\beta R + K\beta q} + K\beta(R-1) \right) . \quad (79)$$

The free energy F defined by $Z = \exp(-N\beta nF)$ is therefore given by

$$\begin{aligned} F/(JK) = & \frac{1}{2}m^2 + \frac{a}{2K\beta} \left(\ln(1 - K\beta R + K\beta q) - \frac{K\beta q}{1 - K\beta R + K\beta q} + K\beta(R-1) \right) - \frac{a\beta K}{2}\tilde{q}q + \frac{a\beta K}{2}\tilde{R}R \\ & - \frac{1}{\beta K} \int Dz \ln \int Dw \left((2 \cosh \beta u_+)^K + (2 \cosh \beta u_-)^K \right) . \end{aligned} \quad (80)$$

The consistency equations for q, R, m, \tilde{q} and \tilde{R} are

$$\tilde{q} = \frac{q}{(1 - K\beta(R - q))^2} , \quad (81a)$$

$$\tilde{R} = \frac{q}{(1 - K\beta(R - q))^2} + \frac{R - q}{(1 - K\beta(R - q))} , \quad (81b)$$

$$m = \int Dz Y^{-1} \int Dw \left(\frac{g_+}{u_+} (2 \cosh \beta u_+)^{K-1} (2 \sinh \beta u_+) + \frac{g_-}{u_-} (2 \cosh \beta u_-)^{K-1} (2 \sinh \beta u_-) \right) , \quad (81c)$$

$$q = \int Dz Y^{-2} \int Dw \left[\left(\frac{g_+}{u_+} (2 \cosh \beta u_+)^{K-1} (2 \sinh \beta u_+) \right)^2 + \left(\frac{g_-}{u_-} (2 \cosh \beta u_-)^{K-1} (2 \sinh \beta u_-) \right)^2 \right] , \quad (81d)$$

$$\begin{aligned} R = & \frac{1}{\beta K} \int Dz Y^{-1} \int Dw \left[\beta(K-1) (2 \cosh \beta u_+)^{K-2} (2 \sinh \beta u_+)^2 \left(\frac{g_+}{u_+} \right)^2 + \beta (2 \cosh \beta u_+)^K \left(\frac{g_+}{u_+} \right)^2 \right. \\ & + (2 \cosh \beta u_+)^{K-2} (2 \sinh \beta u_+)^2 \frac{\Gamma^2}{u_+^3} \\ & + \beta(K-1) (2 \cosh \beta u_-)^{K-2} (2 \sinh \beta u_-)^2 \left(\frac{g_-}{u_-} \right)^2 + \beta (2 \cosh \beta u_-)^K \left(\frac{g_-}{u_-} \right)^2 \\ & \left. + (2 \cosh \beta u_-)^{K-2} (2 \sinh \beta u_-)^2 \frac{\Gamma^2}{u_-^3} \right] . \end{aligned} \quad (81e)$$

In the low temperature limit, $R - q$ and $\tilde{R} - \tilde{q}$ go to zero and

$$m \rightarrow \int Dz \frac{g_+}{u_+} , \quad (82a)$$

$$q \rightarrow \int Dz \frac{g_+^2}{u_+^2} , \quad (82b)$$

$$R \rightarrow \int Dz \frac{g_+^2}{u_+^2} , \quad (82c)$$

where

$$g_+ = \left(m + \gamma + \sqrt{a\tilde{q}z} \right) , \quad (83a)$$

$$u_+ = \sqrt{g_+^2 + \Gamma^2} , \quad (83b)$$

$$Y = (2 \cosh \beta u_+)^K , \quad (83c)$$

and we have defined

$$\lim_{\beta \rightarrow \infty} \beta K(R - q) = \int Dz \frac{\Gamma^2}{u_+^3} = C . \quad (84)$$

The free energy in the limit $\beta \rightarrow \infty$ is

$$F/(JK) = \frac{1}{2}m^2 + \frac{a}{2} \left(-1 + \frac{qC}{(1-C)^2} \right) - \int Dz \sqrt{\left(m + \gamma + \sqrt{a \frac{q}{(1-C)^2} z} \right)^2 + \Gamma^2} . \quad (85a)$$

We show examples of consistent solutions in Fig. 13.

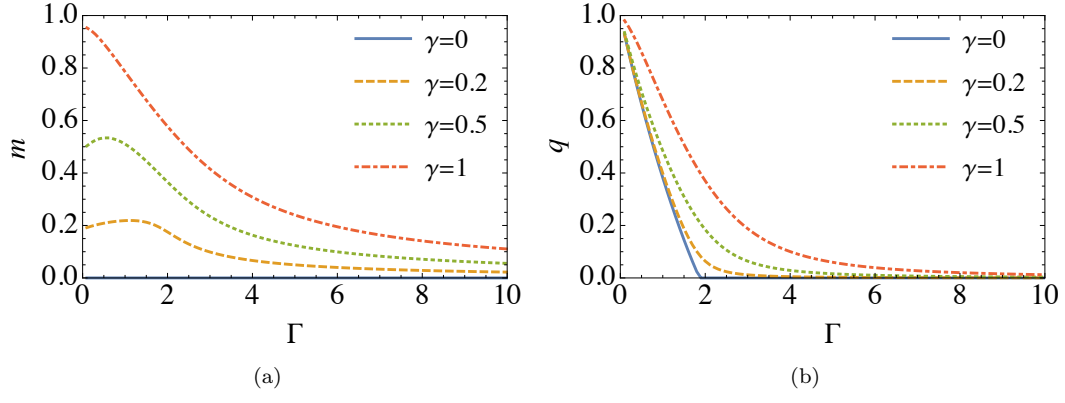


FIG. 13. Behavior of m (a) and q (b) for the Hopfield model with $p = 2$ and many patterns embedded at $R = 0.25N$ and $K = 3$.